cmgh
CELLULAR AND MOLECULAR GASTROENTEROLOGY AND HEPATOLOGY

ORIGINAL RESEARCH

Goblet Cell Loss Linked to NOD2 and Secondary Resection in Crohn's Disease Is Induced by Dysbiosis and Epithelial MyD88

Serre-Yu Wong,[1] Maria Manuela Estevinho,[2,3] Thomas Heaney,[4] Allison A. Marshall,[5] Elisabeth Giselbrecht,[1] Scott G. Daniel,[6] Chaoting Zhou,[7,8] Adriana Rosas-Villegas,[4,9] Kyung Ku Jang,[10,11] Hairu Yang,[8] Huaibin Mabel Ko,[12,13] John D. Paulsen,[12] Yi Ding,[14] Kyle Bittinger,[6] Judy H. Cho,[12] James D. Lewis,[8,15,16] Deepshika Ramanan,[4,17] and Ken Cadwell[8,18]

[1]The Henry D. Janowitz Division of Gastroenterology, Icahn School of Medicine at Mount Sinai, New York, New York; [2]Department of Gastroenterology, Unidade Local de Saúde Gaia Espinho, Vila Nova de Gaia, Portugal; [3]Department of Biomedicine, Unit of Pharmacology and Therapeutics, Faculty of Medicine, University of Porto, Porto, Portugal; [4]Skirball Institute of Biomolecular Medicine, New York University Grossman School of Medicine, New York, New York; [5]Department of Medicine, Icahn School of Medicine at Mount Sinai, New York; [6]Division of Gastroenterology, Hepatology and Nutrition, Children's Hospital of Philadelphia, Philadelphia, Pennsylvania; [7]Cell and Molecular Biology Graduate Program, University of Pennsylvania Perelman School of Medicine, Philadelphia, Pennsylvania; [8]Division of Gastroenterology and Hepatology, Department of Medicine, University of Pennsylvania Perelman School of Medicine, Philadelphia, Pennsylvania; [9]Laboratory of Neurogenetics and Behavior, The Rockefeller University, New York, New York; [10]Department of Microbiology, New York University Grossman School of Medicine, New York, New York; [11]Department of Anatomy, Yonsei University College of Medicine, Seoul, Republic of Korea; [12]Department of Pathology, Molecular & Cell-Based Medicine, Icahn School of Medicine at Mount Sinai, New York, New York; [13]Department of Pathology and Cell Biology, Columbia University Irving Medical Center, New York, New York; [14]Department of Laboratory Medicine, Geisinger Medical Center, Danville, Pennsylvania; [15]Department of Biostatistics, Epidemiology and Informatics, Perelman School of Medicine, University of Pennsylvania, Philadelphia, Pennsylvania; [16]Center for Clinical Epidemiology and Biostatistics, Perelman School of Medicine, University of Pennsylvania, Philadelphia, Pennsylvania; [17]NOMIS Center for Immunobiology and Microbial Pathogenesis, Salk Institute for Biological Studies, La Jolla, California; and [18]Department of Pathobiology, University of Pennsylvania Perelman School of Veterinary Medicine, Philadelphia, Pennsylvania

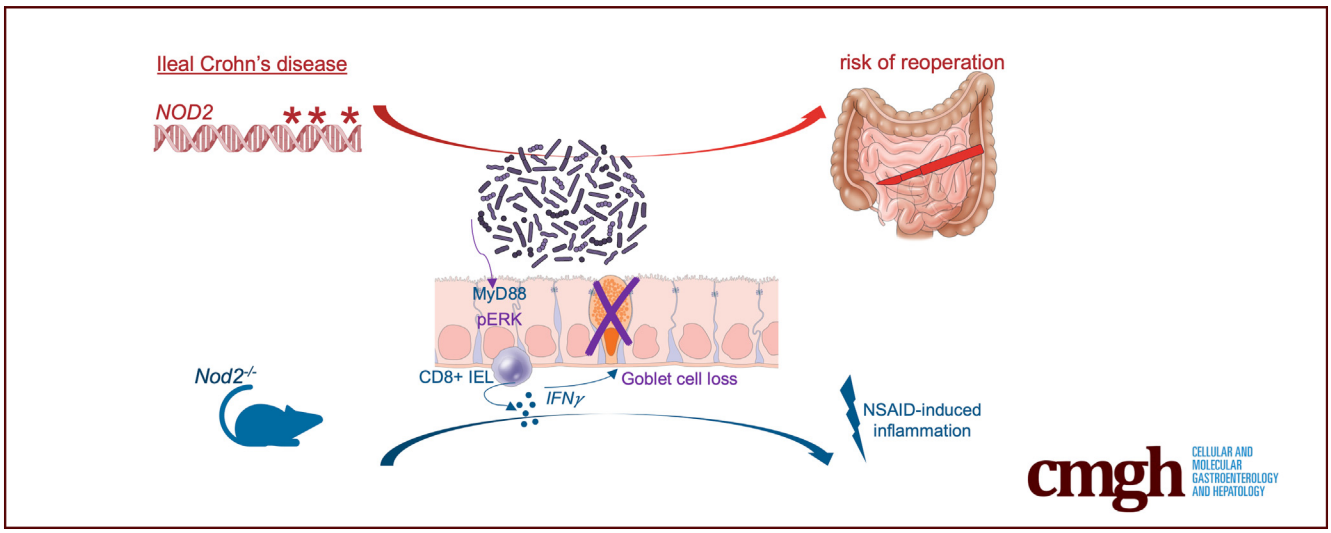

SUMMARY

We show that *NOD2* risk alleles associate with ileal goblet cell loss and increased need for reoperation in patients with Crohn's disease. Mouse models and supporting data from human cohorts indicate that this defect is driven by microbiota dysbiosis and epithelial innate immune signaling.

BACKGROUND & AIMS: The role of goblet cells in small intestinal inflammation in Crohn's disease (CD) is unknown. Polymorphisms of *NOD2* confer risk for CD and associate with small intestinal disease location. We previously showed in mice that *Nod2* deficiency leads to overexpansion of *Phocaeicola vulgatus* in the gut and downstream goblet cell defects, which preceded small intestinal inflammation. In this study, we ask whether goblet cell defects occur in patients with CD with

NOD2 polymorphisms and investigate in mice how *P vulgatus* signals through the intestinal epithelium.

METHODS: We performed a retrospective study of patients with CD to assess clinical outcomes and goblet cell histology by *NOD2* status. We evaluated the contribution of microbiota and MyD88 signaling in the intestinal epithelium to goblet cell defects in the setting of *Nod2* deficiency using genetic mouse models and germ-free mice.

RESULTS: In patients with CD who have undergone ileocolic resection, *NOD2* risk alleles confer a risk for reoperation (odds ratio, 8.12; $P = .047$) and for increased phosphorylated extracellular signal-regulated kinase and goblet cell defects in uninflamed ileal tissue. We show that patients with CD with ileal involvement harbor *P vulgatus* regardless of *NOD2* risk allele status. We show that intestinal epithelial MyD88 and TLR4 are required for goblet cell defects in *Nod2*$^{-/-}$ mice harboring *P vulgatus*. Finally, we show that *P vulgatus* requires complex microbiota to exert its effects in *Nod2*-deficient mice.

CONCLUSIONS: Goblet cell defects may be a harbinger of small intestinal inflammation in patients with CD, particularly in the postoperative setting. Our findings in mice show that small intestinal goblet cell loss associated with *Nod2* mutation is induced by microbiome dysbiosis and epithelial MyD88, in part due to TLR4 signaling. *(Cell Mol Gastroenterol Hepatol 2025; 19:101533; https://doi.org/10.1016/j.jcmgh.2025.101533)*

Keywords: Crohn's Disease; Goblet Cells; Intestinal Epithelium; Microbiota Dysbiosis; NOD2; TLR4.

In the gastrointestinal tract, the host intestinal epithelium and overlying mucus layer are in direct juxtaposition with a diverse microbial ecosystem. The host derives myriad benefits from this interaction, including nutrient generation and absorption and resistance to colonization by potential pathogens.[1–3] Disruption of this homeostasis and intestinal inflammation occurs in inflammatory bowel disease (IBD), including ulcerative colitis (UC) and Crohn's disease (CD).[4] The etiology of IBD is multifactorial, with contributions of host genetic factors, host immune system, environment, and microbiota.[5,6]

Compared with studies of inflammation in the colon, studies highlighting pathways to small intestinal inflammation are relatively scarce. This distinction is important because CD and UC are different in both anatomy and behavior: CD includes transmural inflammation anywhere along the gastrointestinal tract, whereas UC is limited to the mucosal layer of the colon. There are also known functional and microbial community differences along the gastrointestinal tract. Thus, understanding pathways to inflammation at different anatomic sites may hold important clues to understanding the etiology of these diseases.

Goblet cells throughout the epithelium secrete mucus that forms a chemical-physical barrier between gut microbes and their hosts. Mucins, the glycoproteins that form this mucus layer, are diminished in patients with UC and CD.[7–11] Goblet cell numbers, normally most abundant in the colon, are depleted in inflamed colonic sections, particularly affecting patients with UC.[12] Another study using colonoids from patients with UC showed an abnormal phenotype, including failure to secrete mucin in response to agonists.[13] The nature of mucus abnormalities in the colon of patients with CD is less clear, with some studies reporting a lack of goblet cell depletion, consistent with distinct pathogenesis mechanisms underlying IBD subsets.[14,15] Goblet cell numbers and characteristics have not been well-described in small intestinal tissue of patients with CD.

Mutations in *NOD2* confer the highest risk for CD and are associated with disease location in the small intestine.[16,17] Whether *NOD2* risk alleles are associated with specific disease outcomes has been queried but remains debated.[18] For instance, although a recent meta-analysis solidified *NOD2* alleles as risk factors for disease recurrence after surgery, their roles in risk of reoperation remains contested.[18,19] *NOD2* encodes an intracellular protein that is activated by muramyl dipeptide derived from peptidoglycan, which is part of the cell wall of both Gram-positive and Gram-negative bacteria. The 3 main *NOD2* risk alleles for CD are associated with reduced activation in cell culture assays and mouse models.[20–27] NOD2 functions in both hematopoietic and nonhematopoietic cells and is necessary to control infections by pathogenic microbes.[28,29] Deficient NOD2 function has been linked to microbiota dysbiosis in mice and humans.[30–32] This role may be particularly important for understanding IBD, as one proposed mechanism involves a breakdown in tolerance to microbes.

We previously showed that *Nod2* deficiency in mice leads to overexpansion of the commensal *Phocaeicola vulgatus* (formerly *Bacteroides vulgatus*), subsequent goblet cell defects, and susceptibility to inflammation in the small intestine.[33,34] We subsequently demonstrated that helminth infection can protect against this susceptibility via changes to the microbiota that resist *Bacteroidales* (including *Phocaeicola* and *Bacteroides*) colonization that occur in both mice and humans and rely on type 2 immunity.[34] Moreover, the goblet cell defects are dependent upon production of interferon-ɣ (IFNɣ) from CD8+ intraepithelial lymphocytes

Abbreviations used in this paper: **ANOVA, analysis of variance; B6, C57BL/6J; BBE, Bacteroides bile esculin; BHI, brain heart infusion; BM, bone marrow; CD, Crohn's disease; CFU, colony forming unit; DTT, dithiothreitol; EDTA, ethylenediaminetetraacetic acid; FDR, false discovery rate; FFPE, formalin-fixed paraffin-embedded; GF, germ-free; H&E, hematoxylin and eosin; HBSS, Hanks' Balanced Salt Solution; IBD, inflammatory bowel disease; IEC, intestinal epithelial cell; IEL, intraepithelial lymphocyte; IFN- ɣ, interferon-ɣ; IHC, immunohistochemistry; IQR, interquartile range; ISMMS, Icahn School of Medicine at Mount Sinai; LPS, lipopolysaccharide; MRS, de Man-Rogosa-Sharpe agar; NSAID, nonsteroidal anti-inflammatory drug; NYU, New York University; PAS, periodic acid-Schiff; PBS, phosphate buffered saline; pERK, phosphorylated extracellular signal-regulated kinase; PMA, phorbol 12-myristate 13-acetate; PYG, peptone yeast extract glucose; SNP, single nucleotide polymorphism; SPF, specific pathogen-free; TLR, toll-like receptor; TSB, tryptic soy broth; UC, ulcerative colitis; WT, wild-type.**

Most current article

2352-345X
https://doi.org/10.1016/j.jcmgh.2025.101533

(IELs). From bone marrow (BM) chimera experiments, our findings showed that *Nod2* deficiency from BM-derived cells were sufficient to allow for *P vulgatus* colonization. However, in our model the defects ultimately occur in the epithelium, and the contribution of NOD2 to goblet cell defects remains undefined.

In this study, we investigate how defective NOD2 leads to loss of tolerance to *P vulgatus*, resulting in small intestinal goblet cell defects. To address this, we analyzed clinical characteristics and outcomes of a cohort of patients with CD according to *NOD2* risk allele status. In a subset of these patients who underwent ileocolic resection, we correlate *NOD2* risk allele status with goblet cell defects in uninflamed ileum. In a second patient cohort, we confirm *P vulgatus* presence in patients with CD with ileal disease. Next, we probe the toll-like receptor (TLR) pathway and cell-types through which *P vulgatus* initiates pathogenic events in *Nod2*-deficient mice. We show evidence for phosphorylated extracellular signal-regulated kinase (pERK), one of the downstream mediators of MyD88, in the intestinal epithelium of both mice and patients and confirm a requirement for MyD88 in intestinal epithelial cells (IECs) in cell-type specific knockout mice. We find that deletion of TLR4 abrogates small intestinal defects in this model, thereby suggesting that aberrant MyD88 signaling in the setting of *Nod2* deficiency is induced by TLR4 engagement in IECs. Finally, in germ-free mouse experiments, we show that *P vulgatus* is necessary but not sufficient to induce goblet cell defects in *Nod2*-deficient mice; rather, it requires the presence of commensals.

Results

NOD2 Risk Alleles Are Associated With Fistulizing Disease and Reoperation in Patients With Crohn's Disease

Of 106 patients who underwent genotyping for the 3 major CD-associated *NOD2* risk alleles at the Icahn School of Medicine at Mount Sinai (ISMMS), 61 harbored no risk alleles and 45 carried 1 or 2 risk alleles (Table 1). Among the cases, 34 individuals had 1 risk allele, and 11 had 2 risk alleles, including 7 homozygotes and 4 compound heterozygotes. We performed retrospective chart review of these patients. Demographic and disease-related characteristics are shown in Table 2.

Univariate analysis revealed that cases and controls were similar for all baseline characteristics except for age at diagnosis and disease phenotype. Patients carrying *NOD2* risk alleles were younger at diagnosis (median age of 22 [interquartile range (IQR) 11] vs 27 [IQR, 18] years; $P = .048$) and more likely to have penetrating disease (46.7% vs 16.4%; $P = .003$). No differences were observed in remaining demographics when comparing patients with or without *NOD2* risk alleles ($P > .05$ for all characteristics) (Table 2).

Analysis of disease outcomes showed that patients with CD carrying *NOD2* risk alleles were more likely to require biologics or small molecules during disease course (73.3% vs 52.5%; $P = .043$). The rates of abdominal surgery for CD were not different between *NOD2* risk allele carriers and non-risk allele *NOD2* patients (66.7% vs 75.4%; $P = .187$) (Table 2). However, individuals carrying *NOD2* risk alleles were more likely to have negative postoperative disease outcomes, including recurrence of disease (55.6% vs 42.5%; $P = .008$), need for postoperative advanced therapy (42.2% vs 29.5%; $P = .026$), reoperation (40% vs 23%; $P = .01$), and hospitalization (42.2% vs 29.5%; $P = .041$) (Table 2). No statistical differences were identified in patients with 1 or 2 risk alleles ($P > .05$) (Supplementary Table 1). On multivariate analysis and after adjustment for age and disease duration, only the odds ratio (OR) for need for reoperation remained significant (OR, 6.78; 95% confidence interval [CI], 1.05–26.12; $P = .048$) (Supplementary Table 2).

Table 1. Distribution of *NOD2* Risk Alleles in the ISMMS Patient Cohort

Genotype	Patients, *n* (%)[a]
No risk allele	61 (57.5)
Single risk allele	
G908R.rs2066845	18 (17.0)
R702W.rs2066844	5 (4.7)
X1007fs.rs5743293	11 (10.4)
Two risk alleles - homozygotes	
G908R.rs2066845	3 (2.8)
R702W.rs2066844	2 (1.9)
X1007fs.rs5743293	2 (1.9)
Two risk alleles - compound heterozygotes	
G908R.rs2066845 * R702W.rs2066844	1 (0.9)
G908R.rs2066845 * X1007fs.rs5743293	3 (2.8)

ISMMS, Icahn School of Medicine at Mount Sinai.
[a]Percentage of the entire cohort (n=106)

NOD2 Risk Allele Status Is Associated With Goblet Cell Defects in Noninflamed Ileal Sections From Patients With Crohn's Disease

We previously showed that *Nod2*-deficient mice display a reduction in number and staining intensity by periodic acid-Schiff (PAS)-Alcian blue of goblet cells in small intestinal villi but not crypts.[33,34] These findings were confirmed by transmission electron microscopy demonstrating fewer mucin granules per goblet cell and gene expression analysis showing a decrease in Muc2 expression in *Nod2*-deficient mice.[33,34] We therefore asked whether similar goblet cell abnormalities could be found in patients with defective *NOD2* genes.

We focused on patients with ileal CD who underwent ileocolic resection due to the availability of tissue sections from the surgery that facilitate quantification of goblet cells in well-oriented villi and crypts from the intestinal region of interest. We identified 9 patients with 0 *NOD2* risk alleles, 5 patients with 1 *NOD2* risk allele, and 8 patients with 2 *NOD2* risk alleles for whom formalin-fixed ileocecal resection specimens were available (Figure 1*A*). The patients in the single *NOD2* risk allele group included patients heterozygous for L1007fs. As goblet cell defects in *Nod2*-deficient mice occur in the absence of overt inflammation, we evaluated normal ileal tissue from the negative or minimally

Table 2. Demographic and Clinical Characteristics of a Single-center Cohort of Patients With CD by *NOD2* Risk Allele Status

	WT *NOD2* (n = 61)	*NOD2* risk allele carrier (n = 45)	*P*-value (univariate)
Age at genotyping, *y*	51.0 (24.5)	47.5 (25.5)	.902
Age at diagnosis, *y*	27.0 (18.0)	22.0 (11.0)	.048
Sex at birth - female	30 (49.2)	23 (51.1)	.556
Race			.309
White	58 (95.1)	43 (95.6)	
Black	2 (3.3)	1 (2.2)	
Asian	1 (1.6)	1 (2.2)	
BMI, kg/m^2	24.0 (7.5)	23.0 (5.0)	.357
Smoking status			.496
Current	3 (4.9)	2 (4.4)	
Former	12 (16.7)	9 (20.0)	
Never	46 (75.4)	34 (75.6)	
IBD family history (FDR)	10 (16.4)	11 (24.4)	.109
Disease duration, *y*	18.0 (13.0)	24.0 (17.5)	.070
Montreal classification			
A1	10 (16.4)	13 (28.9)	.302
A2	42 (68.9)	26 (57.8)	
A3	9 (14.8)	6 (13.3)	
L1	21 (34.4)	23 (51.1)	.127
L2	10 (16.4)	3 (6.7)	
L3	30 (49.2)	19 (42.2)	
Perianal	14 (23.0)	15 (33.3)	.302
B1	21 (34.4)	11 (24.4)	.003
B2	30 (49.2)	13 (28.9)	
B3	10 (16.4)	21 (46.7)	
Medication history			
Corticosteroids	52 (85.2)	37 (82.2)	.909
Immunomodulators	29 (47.5)	26 (57.8)	.215
Advanced therapy[a]	32 (52.5)	33 (73.3)	.043
More than 2 advanced therapies	5 (8.2)	7 (15.5)	.129
Surgery - yes	47 (75.4)	30 (66.7)	.187
Ileocolic resection	35 (57.4)	24 (53.3)	.334
Small bowel resection	5 (8.2)	4 (8.9)	
Segmental colectomy	3 (6.6)	0 (0.0)	
Proctocolectomy	2 (3.3)	1 (2.2)	
Time since diagnosis, *y*	6.5 (10.5)	8.0 (9.0)	.353
Postoperative outcomes			
Postoperative recurrence[b]	26 (42.6)	25 (55.6)	.008
Need for advanced therapy after surgery	18 (29.5)	19 (42.2)	.026
Reoperation	14 (23.0)	18 (40.0)	.010
Hospitalization	18 (29.5)	19 (42.2)	.041

Note: Data are presented as number (%) or median (interquartile range).
FDR, first-degree relative; IBD, inflammatory bowel disease; WT, wild-type.
[a]Infliximab, adalimumab, certolizumab, vedolizumab, ustekinumab, rizankizumab, filgotinib, upadacitinib.
[b]Postoperative recurrence was defined using endoscopy (Rutgeerts score ≥i2 for patients with ileocecal resection) or imaging studies (active inflammation in computed tomography or magnetic resonance, as defined in the Methodology section).

inflamed margins of the resections using PAS-Alcian blue staining to highlight the goblet cells (Figure 1*B*). The overall total goblet cell numbers per villus were not significantly different between groups.

However, there were fewer normal goblet cells, defined by staining intensity, in patients harboring *NOD2* risk alleles, with 2 risk alleles having a greater effect than 1 (Figure 1*B* and *E*). Indeed, the ratio of abnormal goblet cells with decreased staining intensity to normal goblet cells increased proportionally compared with the number of *NOD2* risk alleles (Figure 1*F*). In comparison, patients with no risk alleles and non-IBD controls who had undergone ileocecal resection for colon cancer showed no difference in abnormal goblet cell ratios, although the number of normal goblet cells was lower in all patients with CD compared with controls (Figure 1*C* and *F*). To verify results obtained with PAS-Alcian blue, we stained the same sections for MUC2 by immunohistochemistry (IHC) (Figure 1*C*). Although there were no overall differences in total numbers of MUC2+ cells, the ratio of abnormal to normal goblet cells was significantly greater in patients carrying 2 *NOD2* risk alleles (Figure 1*G–I*). These data suggest that mutations in *NOD2* are associated with similar goblet cell defects in both humans and mice.

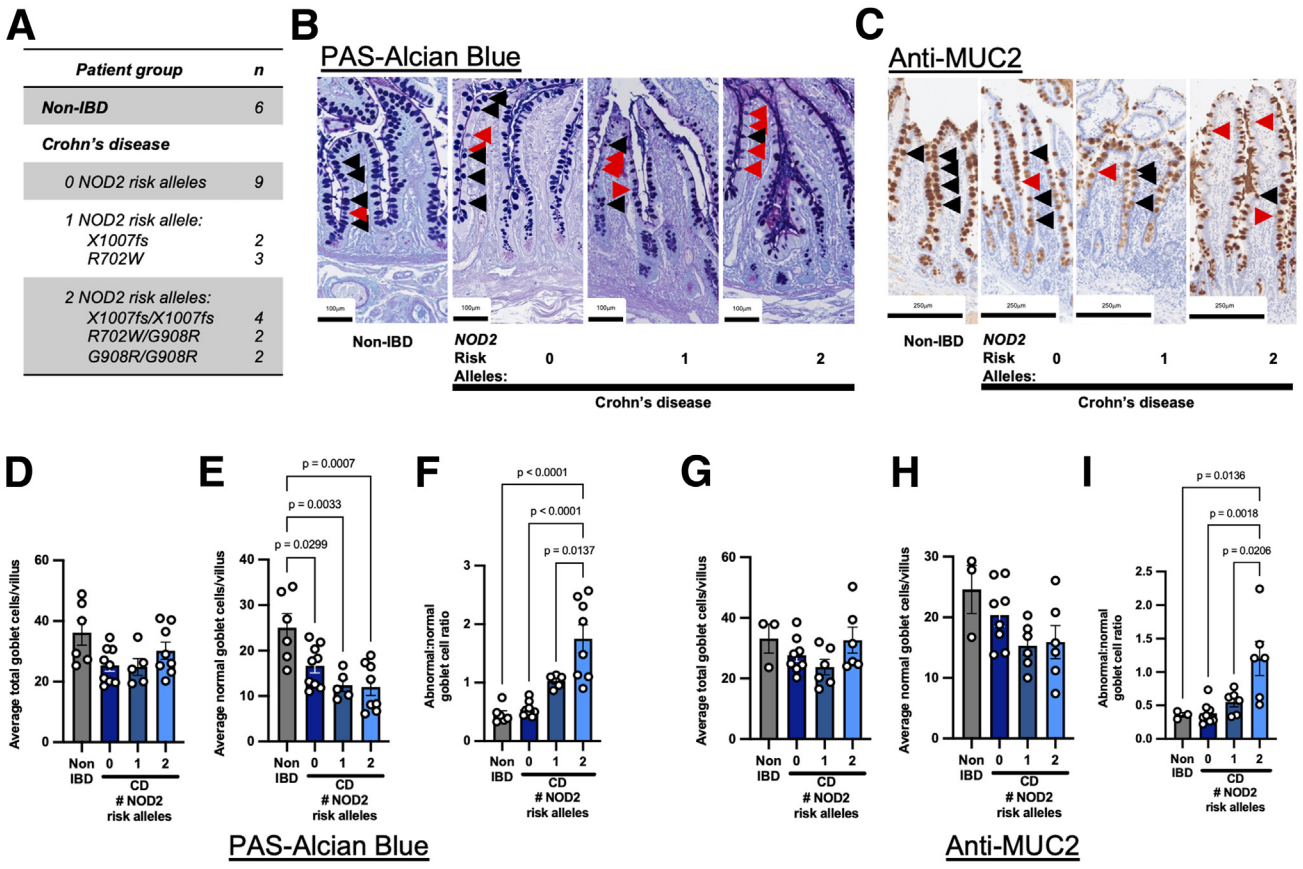

Figure 1. Patients with CD with NOD2 risk alleles display goblet cell abnormalities in the ileum. (*A*) Table of patient groups used for this study. Distribution of NOD2 risk alleles amongst patients with CD: X1007fs (rs5743293), R702W (rs2066844), and G908R (rs2066845). (*B*) Representative PAS-Alcian Blue staining of terminal ileum sections from non-IBD patients who underwent resection for right-sided colon cancer and non-diseased margins of ileocolic resections from patients with CD with 0, 1, or 2 NOD2 risk alleles. Normal goblet cells containing mucin stain *dark blue* (examples indicated by *black arrowheads*). Abnormal goblet cells (examples indicated by *red arrowheads*) were defined by reduced staining intensity by PAS-Alcian blue.[33] Images were taken at 12× magnification. (*C*) Representative MUC2 staining of sections from the same patients by risk allele status. Normal goblet cells containing mucin stain homoegenously *dark brown* (examples indicated by *black arrowheads*). Abnormal goblet cells (examples indicated by *red arrowheads*) were defined by reduced staining intensity by anti-MUC2 antibody. Images were taken at 10× magnification. (*D–F*) Average total number of goblet cells counted per villus, average number of normal goblet cells counted per villus, and ratio of abnormal to normal goblet cells by PAS-Alcian Blue (*G–I*) Average total number of goblet cells counted per villus, average number of normal goblet cells counted per villus, and ratio of abnormal to normal goblet cells by MUC2 staining. Each dot represents values from one patient. Nine to 75 villi (average, 36 villi) were quantified per patient. Ordinary 1-way ANOVA with testing for multiple comparisons (Tukey) was performed with *P*-values $< .05$ shown.

P vulgatus *in Patients With Crohn's Disease by NOD2 Risk Allele Status*

Our previous work showed that small intestinal goblet cell defects in *Nod2*-deficient mice were dependent on overexpansion of *P vulgatus*. We asked whether *P vulgatus* is present in patients with Crohn's disease by *NOD2* risk allele status through analysis of data from the Study of a Prospective Adult Research Cohort with Inflammatory Bowel Disease (SPARC IBD) cohort.[35,36] SPARC IBD is a prospective observational study of patients with IBD throughout the United States, wherein patients provide blood, stool, and intestinal biopsies. Thus, there were available clinical data including surgical history, genetic data, and microbiome data. We evaluated a subcohort of patients who had ileal involvement by excluding those with colonic disease and assessed *NOD2* risk allele status (Figure 2*A*). There were a total of 171 patients, of whom 119 patients had 0 risk alleles, 51 patients had 1 risk allele, and 11 patients had 2 risk alleles. There were no patients carrying rs2066844. Figure 2*A* displays patients by *NOD2* risk allele status and intestinal resection status. Similar to the ISMMS cohort, 2 risk allele status appeared to be higher risk for surgery than 0 and 1 risk alleles combined ($P = .017$).

When we assessed fecal microbiome composition, we found a significant difference in alpha diversity by Shannon diversity index for 1 risk allele (Richness $P = .18$; Shannon $P = .036$) but not 2 risk alleles (Richness $P = .18$; Shannon

A

Genotype (n = 171)	History of intestinal resection	
	yes	no
No risk allele, n (%)	57/119 (47.9%)	62/119 (52.1%)
Single risk allele		
G908R.rs2066845	16	9
R702W.rs2066844	0	0
X1007fs.rs5743293	9	7
All single risk allele, n (%)	25/41 (61%)	16/41 (39%)
Two risk alleles		
Homozygotes	1	2
G908R.rs2066845	0	0
R702W.rs2066844	1	0
X1007fs.rs5743293		
Compound heterozygotes		
G908R.rs2066845 * X1007fs.rs5743293	7	0
All two risk alleles, n (%)	9/11 (81.8%)	2/11 (18.2%)

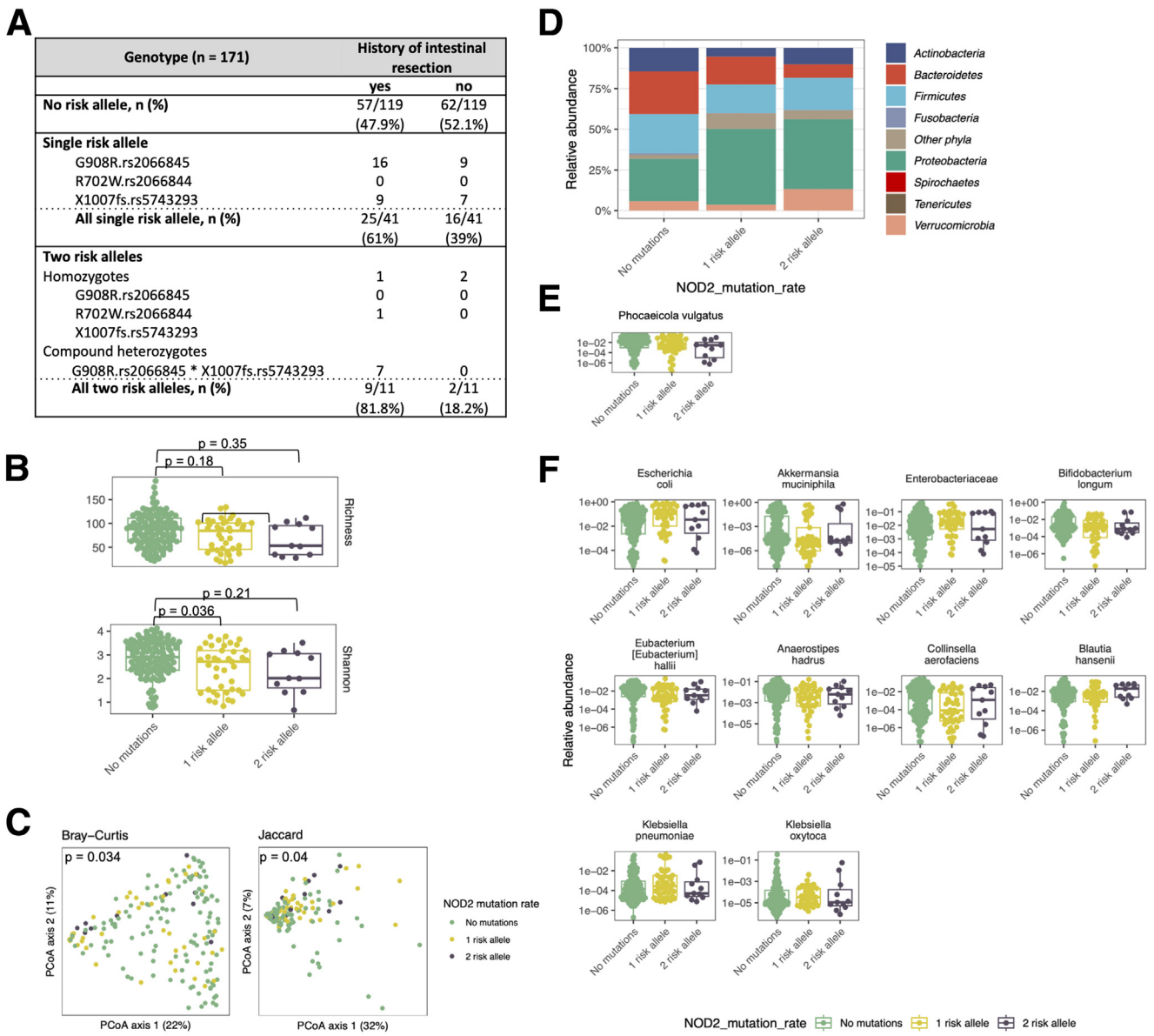

Figure 2. SPARC-IBD cohort association between microbiota and *NOD2* risk allele status in patients with CD with ileal involvement. (*A*) Table of patients with ileal or ileocolonic CD from the SPARC-IBD cohort by NOD2 risk allele status and surgical status. (*B*) Species richness and Shannon diversity index by risk allele status. (*C*) Bray-Curtis and Jaccard plots of samples by risk allele status. (*D*) Relative abundances of fecal microbiota by phyla and according to *NOD2* risk allele status. (*E*) *P vulgatus* abundance by *NOD2* risk allele status. (*F*) Species with increasing abundance by *NOD2* risk allele status. All taxa shown, including *P vulgatus*, are those with >1% mean abundance across samples. Taxa abundances that had zero values were replaced with one-half the minimum value out of all samples for a given taxa.

$P = .21$). Bray Curtis and Jaccard beta diversity were significantly different among groups by risk allele status ($P = .034$ and $P = .04$, respectively) (Figure 2*B* and *C*). There was an increase in phyla *Proteobacteria* and *Verrucomicrobia* (*Akkermanisa muciniphila*) with a decrease in *Bacteroidetes*, which is a distribution that is similar to that of *Nod2*$^{-/-}$ mice after nonsteroidal anti-inflammatory drug (NSAID)-induced inflammation (Figure 2*D*).[33] In mice, *P vulgatus* abundance is increased at baseline in *Nod2*-deficiency but decreases after onset of small intestinal inflammation.[33] In the patient fecal microbiome, *P vulgatus* was identified as one of 21 taxa with a mean relative abundance of >1% across samples (Figure 2*E*). However, it was not significantly associated with risk allele status; species with increasing abundance by *NOD2* risk allele status are shown in Figure 2*F*. Thus, we confirm the presence of *P vulgatus* in the fecal microbiome of patients with ileal CD with and without *NOD2* risk alleles.

Phosphorylated ERK Is Upregulated in Small Intestinal Epithelium of Nod2$^{-/-}$ Mice and Patients With NOD2 Risk Alleles

MyD88 is an intracellular signaling adaptor to TLRs, the family of pattern-recognition receptors that sense microbial-derived products.[37] Our previous analysis of *Nod2*$^{-/-}$*MyD88*$^{-/-}$ mice showed that induction of goblet cell defects by *P vulgatus* is dependent on MyD88.[33] To further link this result to the microbiota, we performed IHC of small intestinal sections from germ-free (GF) *Nod2*$^{-/-}$ mice for pERK as a marker of activation of signaling downstream of MyD88.[38–40] Conventional *Nod2*$^{-/-}$ mice displayed an increase in pERK-positive cells within the intestinal epithelium compared with wild-type (WT) mice, especially in the villi where we previously noted the goblet cell defects. In contrast, GF WT and GF *Nod2*$^{-/-}$ mice displayed low or background levels of pERK staining similar to conventional WT mice (Figure 3*A* and *B*). To assess whether pERK is activated in patients with CD, we stained ileal sections from the ISMMS patient cohort for pERK. Cells that stained darkly positive for pERK were overall sparse (Figure 3*C*). Therefore, we assessed the proportion of villi containing any pERK-positive cells and found significantly increased proportions by risk allele status, specifically associated with 2 risk allele carriers (Figure 3*D*). In contrast to non-IBD and 0 risk allele controls, villi in patients with *NOD2* risk alleles frequently displayed multiple pERK-positive cells per villus (Figure 3*C*). These results indicate that *NOD2* mutation is associated with pERK and raise the possibility that induction of MyD88 pathway signaling occurs in the epithelial compartment in response to the microbiota.

MyD88 in Intestinal Epithelial Cells is Required for Intestinal Abnormalities in Nod2$^{-/-}$ Mice

MyD88 signaling in either lymphoid cells or IECs can regulate IFN-γ expression and goblet cell function.[41–43] Given the epithelial localization of the pERK staining, we hypothesized that MyD88 functions in the IEC compartment of *Nod2*$^{-/-}$ mice in response to overexpansion of *P vulgatus*. To address this, we generated specific deletion of MyD88 in IECs in *Nod2*$^{-/-}$ mice, specifically *Nod2*$^{-/-}$;*MyD88*$^{f/f}$;Villin-cre (*Nod2*$^{-/-}$MyD88$^{\Delta IEC}$). As we have previously reported, *P vulgatus* expansion leads to diminished goblet cells in small intestinal epithelium by both MUC2 and PAS-Alcian blue staining of *Nod2*$^{-/-}$ mice compared with WT mice (Figure 4*A* and *B*).[33] However, *Nod2*$^{-/-}$*MyD88*$^{\Delta IEC}$ mice displayed lower levels of IFN-γ producing CD8+ IELs and no goblet cell abnormalities compared with *Nod2*$^{-/-}$;*MyD88*$^{f/f}$;*Cre-negative* (*Nod2*$^{-/-}$*MyD88*$^{f/f}$) controls (Figure 4*C*). We performed pERK staining in these mice. The *Nod2*$^{-/-}$*MyD88*$^{\Delta IEC}$ mice had fewer pERK cells in small intestinal epithelium similar to WT mice (Figure 4*D*). Thus, Myd88 signaling is required in the IEC compartment to induce intestinal abnormalities observed in *Nod2*$^{-/-}$ mice.

Tlr4 Is Required for P Vulgatus-induced Intestinal Abnormalities in Nod2$^{-/-}$ Mice

Members of the TLR family, for which MyD88 is the canonical intracellular adaptor, recognize an array of conserved microbial structures; intracellular NOD2 recognizes peptidoglycan from bacterial cell walls. Negative crosstalk between NOD2 and TLR2/4 in mice and peripheral blood mononuclear cells have been demonstrated in patients with CD.[44–46] NOD2 and TLRs may also functionally interact within the intestinal epithelium because peptidoglycan can be found along the intestinal epithelial cell lining, and TLRs are variably expressed along the intestinal epithelium.[46,47]

As a Gram-negative bacterium, *P vulgatus* is a source of lipopolysaccharide (LPS) that can activate TLR4. Therefore, we generated *Nod2*$^{-/-}$*Tlr4*$^{-/-}$ mice. These mice displayed more normal goblet cells compared with *Nod2*$^{-/-}$ mice, and the proportion of IFN-γ producing CD8+ IELs was also restored to WT levels in *Nod2*$^{-/-}$*Tlr4*$^{-/-}$ mice (Figure 5*A* and *B*). Given the findings from the *Nod2*$^{-/-}$*MyD88*$^{\Delta IEC}$ mice implicating signaling in IECs, we attempted to generate *Nod2*$^{-/-}$;*Tlr4*$^{f/f}$;*Villin-cre* (*Nod2*$^{-/-}$*Tlr4*$^{\Delta IEC}$) mice. However, offspring from dihybrid crosses with and without Villin-Cre (*Nod2*$^{+/-}$*Tlr4*$^{f/+}$*VillinCre-* x *Nod2*$^{+/-}$*Tlr4*$^{f/+}$*VillinCre+*) did not follow Mendelian ratios after at least 4 test crosses with multiple normal litter sizes (6–12 pups) yielded 1 *Nod2*$^{-/-}$*Tlr4*$^{\Delta IEC}$ mouse. We also attempted *Nod2*$^{+/-}$*Tlr4*$^{f/f}$*VillinCre-* x *Nod2*$^{+/-}$*Tlr4*$^{f/+}$*VillinCre+* and *Nod2*$^{+/-}$*Tlr4*$^{f/f}$*VillinCre+* x *Nod2*$^{-/-}$*Tlr4*$^{f/f}$*VillinCre-*, the latter of which yielded 1 *Nod2*$^{-/-}$*Tlr4*$^{\Delta IEC}$ mouse. Thus, we were unable to produce sufficient numbers of *Nod2*$^{-/-}$*Tlr4*$^{\Delta IEC}$ mice for breeding or experiments.

As an alternate approach, we generated BM chimeras to separate the contribution of TLR4 in hematopoietic cells from radio-resistant cells, which include IECs. NOD2 is required in the hematopoietic compartment to prevent the expansion of *P vulgatus*.[33] Thus, we reconstituted irradiated WT and *Tlr4*$^{-/-}$ mice with BM from *Nod2*$^{-/-}$ mice. Because the mice that we used as recipients of the BM were not colonized with *P vulgatus* at the outset of the experiment, we introduced the bacterium by oral gavage into the chimeric mice. WT and *Tlr4*$^{-/-}$ recipient mice displayed similar stable *P vulgatus* colonization (Figure 5*C*). Analysis of small intestinal tissue showed reduction of both IFN-γ production and goblet cell abnormalities in *Tlr4*$^{-/-}$ mice reconstituted with *Nod2*$^{-/-}$ BM, suggesting that TLR4 signaling in non-hematopoietic radio-resistant cells is necessary for *P vulgatus* to induce small intestinal defects in *Nod2*$^{-/-}$ mice (Figure 5*A* and *B*).

TLR4 levels are very low in the mouse small intestinal epithelium compared with the colonic epithelium, yet the effects of the gut microbiota we find in *Nod2*$^{-/-}$ mice occur in the small intestine.[47] To assess the expression of *Tlr4* in IECs of *Nod2*$^{-/-}$ mice, we harvested Epcam+CD45- IECs from the small intestine and colon of these mice. Colonic tissue of WT and *Nod2*$^{-/-}$ mice showed the highest expression of *Tlr4* by qPCR compared with lower levels in the distal small intestine and little to no expression in the proximal and mid small intestine (Figure 5*D*). These data confirm that TLR4 is present in small quantity in the affected distal small intestine and more abundant in the colon of *Nod2*$^{-/-}$ mice.

Tlr4 and MyD88 Mediate Susceptibility to Small Intestinal Inflammation in Nod2$^{-/-}$ Mice

In the presence of *P vulgatus*, *Nod2*$^{-/-}$ mice are susceptible to small intestinal injury by the NSAID piroxicam.[33]

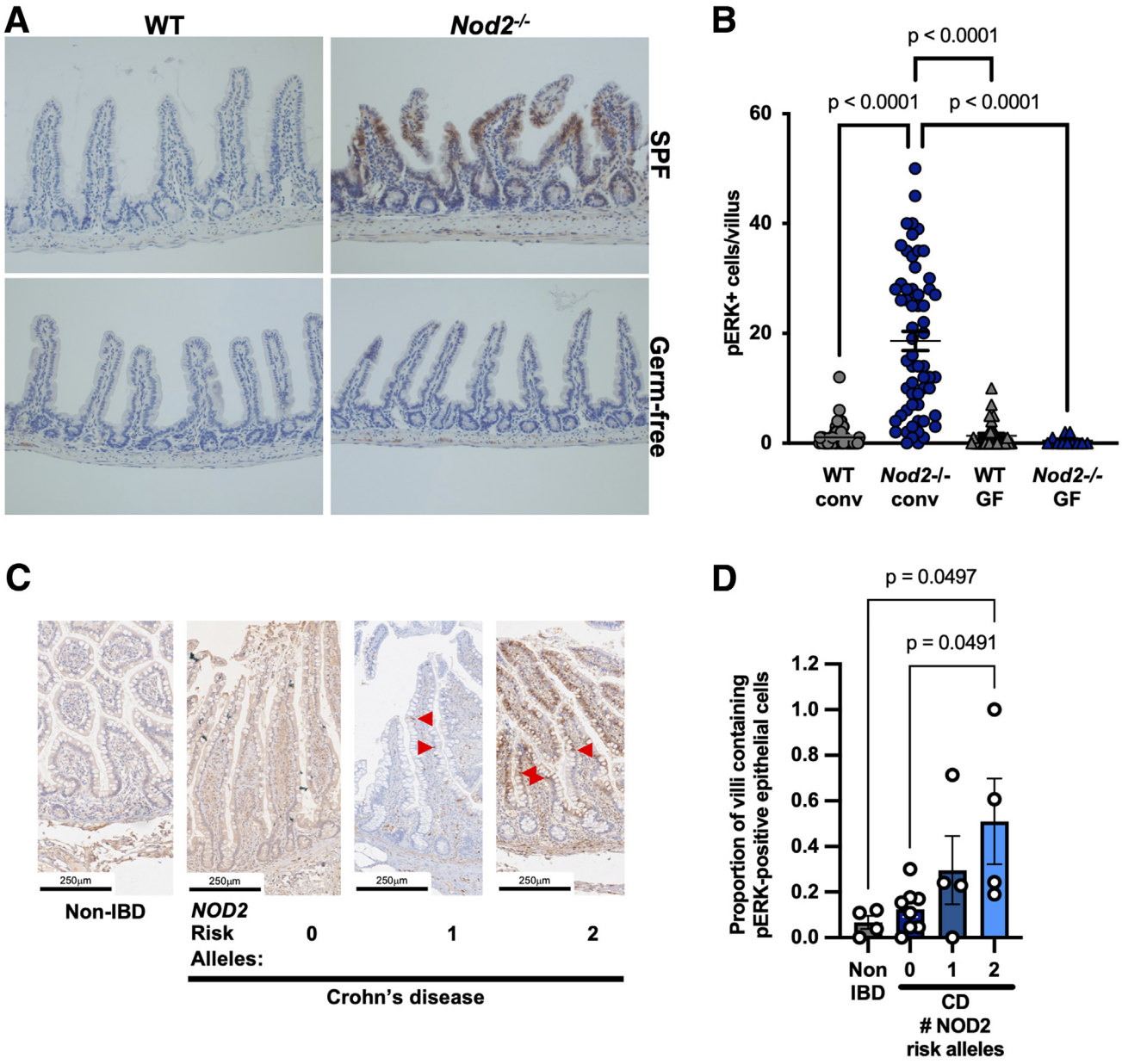

Figure 3. *NOD2* mutation is associated with increases in epithelial pERK in the ileum. (*A*) Representative ileal sections stained with antibodies against pERK from conventional WT and *Nod2*$^{-/-}$ mice and GF WT and *Nod2*$^{-/-}$ mice. (*B*) Quantification of the number of pERK-positive epithelial cells per villus. Ten to 76 villi were quantified per condition. (*C*) Representative ileal sections stained with antibodies against pERK from non-IBD patients who underwent resection for right-sided colon cancer and non-diseased margins of ileocolic resections from patients with CD with 0, 1, or 2 *NOD2* risk alleles. (*D*) Quantification of the proportion of villi containing any pERK-positive cells in patients. N = 331, 758, 478, and 367 villi were examined in non-IBD patients and patients with CD with 0, 1, or 2 *NOD2* risks alleles, respectively. Ordinary 1-way ANOVA with testing for multiple comparisons (Tukey) was performed with *P*-values < .05 shown. Conv = conventional.

Ileal sections from piroxicam-treated *Nod2*$^{-/-}$*MyD88*$^{f/f}$ and *Nod2*$^{-/-}$ mice showed transmural inflammation. In contrast, ileal sections from *Nod2*$^{-/-}$*MyD88*$^{\Delta IEC}$ mice and *Nod2*$^{-/-}$*Tlr4*$^{-/-}$ mice had significantly lower pathology scores and no sections with transmural inflammation, demonstrating that piroxicam-induced intestinal injury is abrogated by loss of TLR4 and loss of MyD88 (Figure 5*E* and *F*). This suggests that the increased susceptibility to small intestinal inflammation observed in *Nod2*$^{-/-}$ mice is dependent on epithelial Tlr4/MyD88 signaling induced by the expansion of *P vulgatus*.

P vulgatus *Is Necessary But Not Sufficient to Induce Small Intestinal Abnormalities in Nod2*$^{-/-}$ *Mice*

Nod2$^{-/-}$ mice purchased from a vendor do not harbor *P vulgatus*.[1,34,48] We bred and maintained these mice

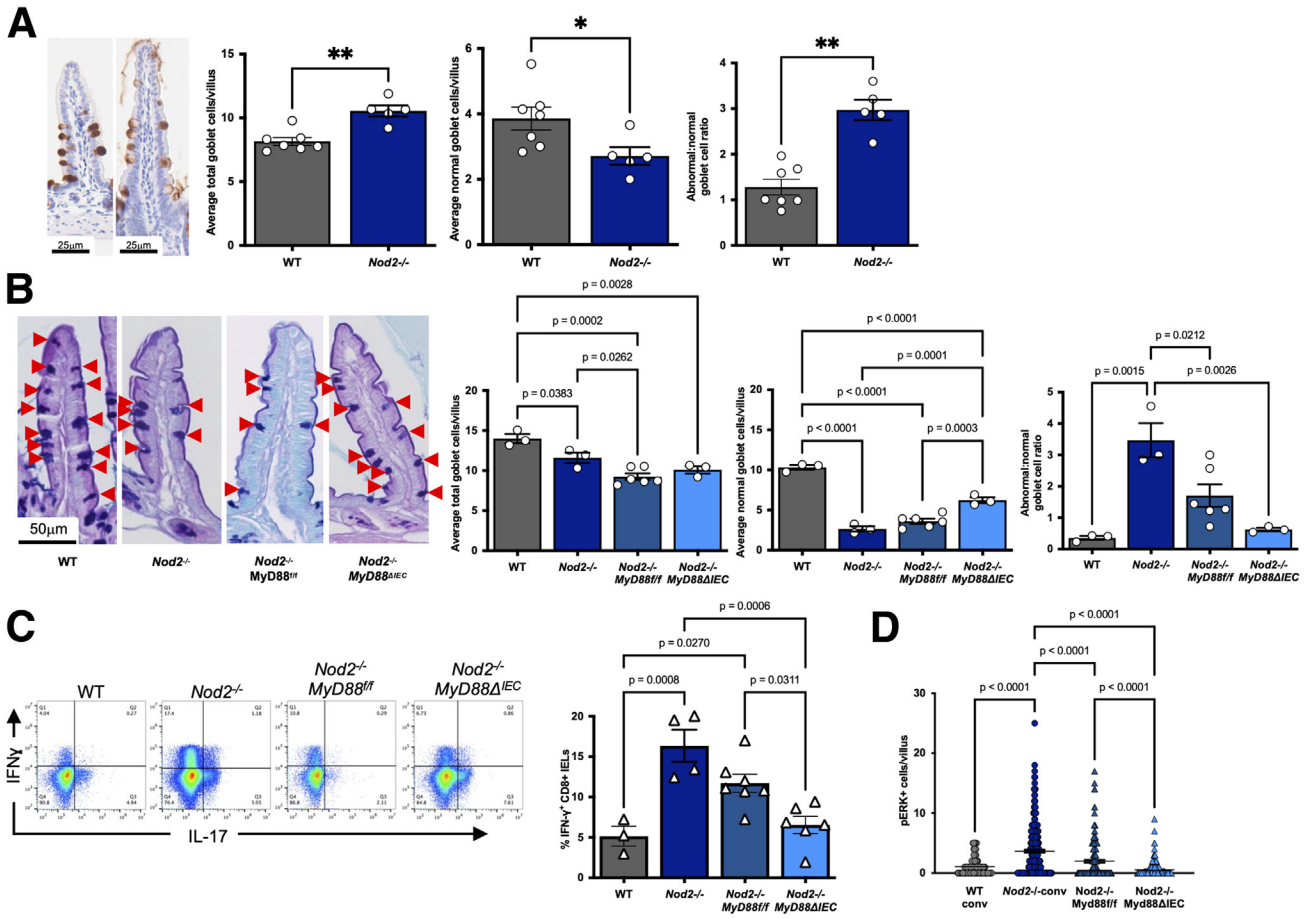

Figure 4. MyD88 signaling in the intestinal epithelium is required for epithelial defects in *Nod2*$^{-/-}$ mice. (*A*) Representative MUC2 staining of sections of ileal sections from WT and *Nod2*$^{-/-}$ mice. Normal goblet cells containing mucin stain homogenously *dark brown* (examples indicated by *black arrowheads*). Abnormal goblet cells (examples indicated by *red arrowheads*) were defined by reduced staining intensity by the GTX100664 anti-MUC2 antibody (GeneTex). Images were taken at 20× magnification. Quantification of the average total number of goblet cells counted per villus, the number of normal goblet cells per villus, and the ratio of abnormal to normal goblet cells WT and *Nod2*$^{-/-}$ mice. (*B*) Representative PAS-Alcian blue staining of ileal sections from WT, *Nod2*$^{-/-}$, *Nod2*$^{-/-}$ *MyD88*$^{f/f}$, and *Nod2*$^{-/-}$*MyD88*$^{\Delta IEC}$ mice (*red arrowheads* denote goblet cells) and quantification of the average total number of goblet cells counted per villus, the number of normal goblet cells per villus, and the ratio of abnormal to normal goblet cells in the same mice. (*C*) Quantification of the percentage of CD8+ IELs expressing IFNγ in WT, *Nod2*$^{-/-}$, *Nod2*$^{-/-}$*MyD88*$^{f/f}$, and *Nod2*$^{-/-}$*MyD88*$^{\Delta IEC}$ mice with representative flow cytometry plot of CD8^{+} IELs from stained for intracellular IFN-γ and IL-17 expression after stimulation with PMA and ionomycin (gated on CD3+ live cells). (*D*) Quantification of the number of pERK-positive epithelial cells per villus, n = 97–287 villi were quantified per condition in WT, *Nod2*$^{-/-}$, *Nod2*$^{-/-}$*MyD88*$^{f/f}$, *Nod2*$^{-/-}$*MyD88*$^{\Delta IEC}$ mice. Representative data from at least 2 independent experiments with n = 3–7 mice/group are shown. At least 25 villi per mouse were quantified for *A* and *B*. Ordinary 1-way ANOVA with testing for multiple comparisons (Holm-Šídák) (*B* and *D*) were performed with *P*-values < .05 shown.

(*Nod2*$^{-/-}$Jax) in a separate room to avoid contact with *P vulgatus*-colonized mice. After confirming absence of colonization (Figure 6*E*), we found that they displayed similar numbers of morphologically normal goblet cells per villus and IFN-γ production by CD8+ IELs as WT mice (Figure 6*A–D*). Following oral gavage with *P vulgatus*, we found that *Nod2*$^{-/-}$Jax mice became readily colonized and displayed abnormalities similar to *Nod2*$^{-/-}$ mice previously raised in our institutional vivarium (Figure 6*A–E*). Thus, *P vulgatus* is necessary for small intestinal abnormalities to occur in *Nod2*$^{-/-}$ mice.

Next, we investigated whether *P vulgatus* colonization is sufficient to induce abnormalities in *Nod2*-deficient hosts. At baseline, small intestinal tissue from GF *Nod2*$^{-/-}$ mice appeared similar to GF WT controls when comparing morphology, goblet cells, and IFN-γ production by CD8+ IELs. Upon oral gavage with *P vulgatus*, GF *Nod2*$^{-/-}$ mice remained stably mono-colonized; yet, we did not detect small intestinal abnormalities in either GF *Nod2*$^{-/-}$ or GF WT mice, including goblet cell defects and IFN-γ production by CD8+ IELs (Figure 6*F–J*). Thus, *P vulgatus* is necessary but not sufficient for these defects to occur in *Nod2*$^{-/-}$ mice.

To test whether other commensals are required for induction of defects via *P vulgatus*, we introduced both *P vulgatus* and stool from conventional *Nod2*$^{-/-}$ mice into GF *Nod2*$^{-/-}$ mice. This combination was able to induce increased

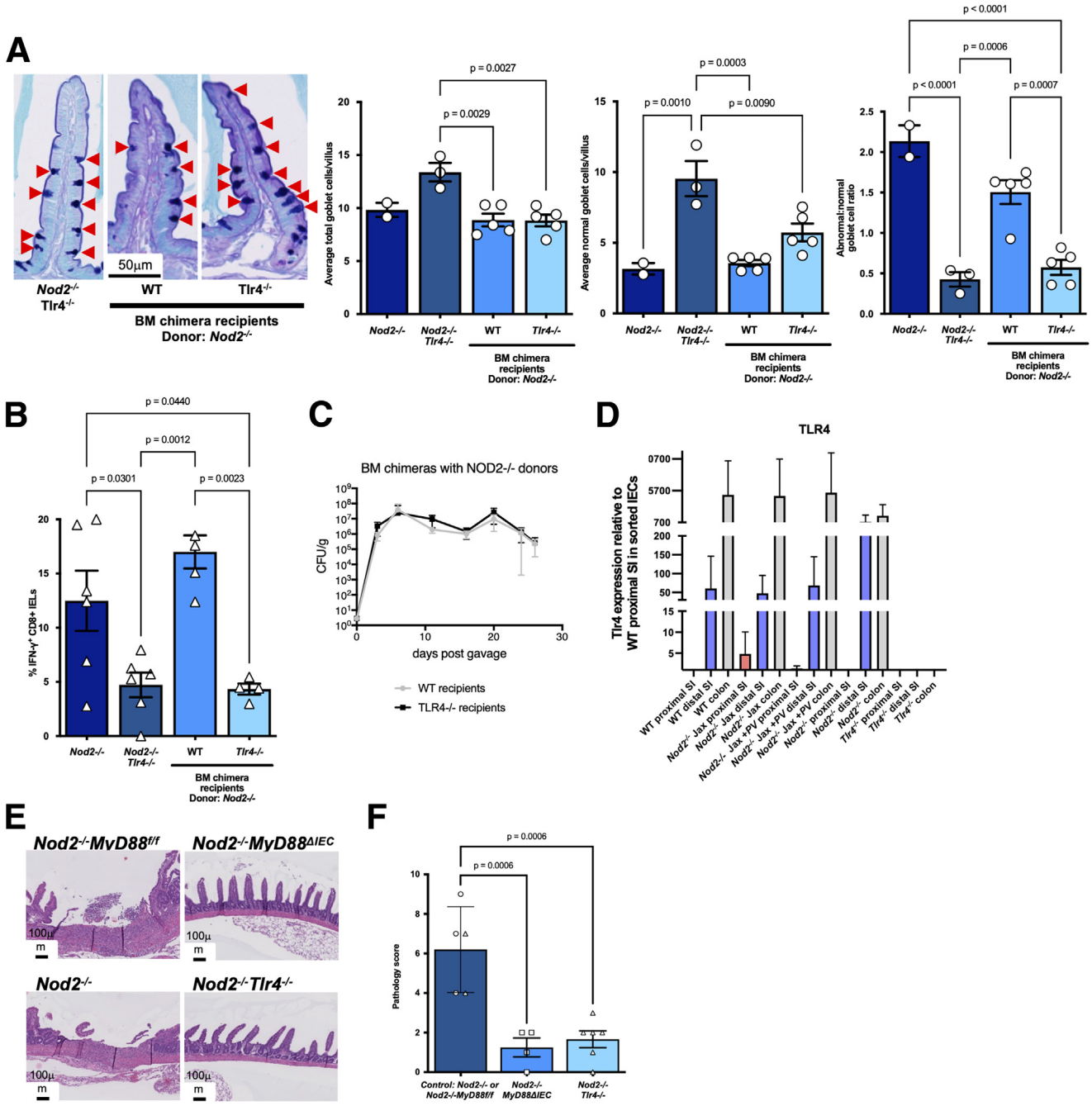

Figure 5. TLR4/MyD88 signaling in the intestinal epithelium is required for inflammatory defects in *Nod2*$^{-/-}$ mice. (*A*) Representative PAS-Alcian blue staining of ileal sections from *Nod2*$^{-/-}$*Tlr4*$^{-/-}$ mice and BM chimeras (donors: *Nod2*$^{-/-}$ mice, recipients: WT and *Tlr4*$^{-/-}$). *Red arrowheads* denote goblet cells. Quantification of the average total number of goblet cells counted per villus, the number of normal goblet cells per villus, and the ratio of abnormal to normal goblet cells in *Nod2*$^{-/-}$, *Nod2*$^{-/-}$*Tlr4*$^{-/-}$ mice and in BM chimeras (donors: *Nod2*$^{-/-}$ mice, recipients: WT and *Tlr4*$^{-/-}$). (*B*) Quantification of the percentage of CD8+ IELs expressing IFNγ in *Nod2*$^{-/-}$ and *Nod2*$^{-/-}$*Tlr4*$^{-/-}$ mice and in BM chimeras (donors: *Nod2*$^{-/-}$ mice, recipients: WT and *Tlr4*$^{-/-}$) after stimulation with PMA and ionomycin. (*C*) CFUs of *P vulgatus* per milligram (mg) of stool collected over time in stool of WT and *Tlr4*$^{-/-}$ mice gavaged with *P vulgatus*. (*D*) Relative expression of Tlr4 by qPCR in IECs sorted from proximal and distal small intestine and colon in WT, *Nod2*$^{-/-}$ Jax, *Nod2*$^{-/-}$ Jax gavaged with *P vulgatus* (PV), and *Tlr4*$^{-/-}$ mice are shown. Expression is shown relative to WT proximal small intestine (WT SI P). (*E*) Representative H&E-stained ileal sections from *Nod2*$^{-/-}$*MyD88*$^{f/f}$, *Nod2*$^{-/-}$*MyD88*$^{\Delta IEC}$, *Nod2*$^{-/-}$, and *Nod2*$^{-/-}$*Tlr4*$^{-/-}$ treated with piroxicam. Sections from *Nod2*$^{-/-}$*MyD88*$^{f/f}$ and *Nod2*$^{-/-}$ each showed several foci of loss of epithelium in a skipping fashion with mixed acute and chronic inflammation through the intestinal wall and thickening of the muscularis layer. Sections from *Nod2*$^{-/-}$*MyD88*$^{\Delta IEC}$ and *Nod2*$^{-/-}$*Tlr4*$^{-/-}$ mice showed no overt inflammation throughout. (*F*) Quantification of small intestinal pathology in mice treated with piroxicam; controls are marked as follows *Nod2*$^{-/-}$ (*clear circles*) and *Nod2*$^{-/-}$*MyD88*$^{f/f}$ (*clear triangles*). Representative data from at least 2 independent experiments with n = 3–7 mice/group are shown. At least 25 villi per mouse were quantified for *A*. Ordinary 1-way ANOVA with testing for multiple comparisons (Holm-Šídák) (*A, B, and F*) were performed with *P*-values < .05 shown.

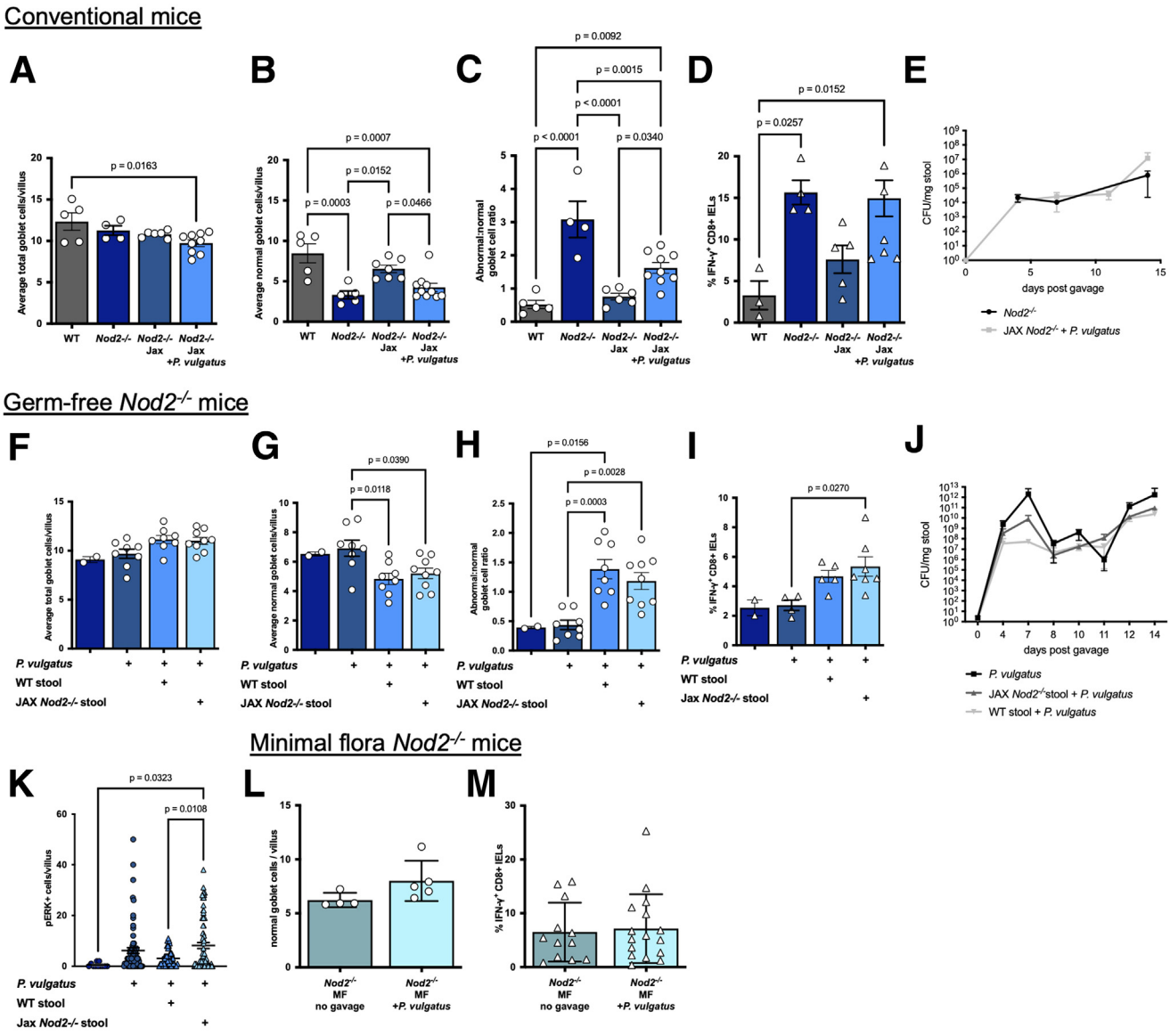

Figure 6. *P vulgatus* is necessary but not sufficient to exert changes in small intestine. (*A–C*) Quantification of the number of total goblet cells per villus, normal goblet cells per villus, and ratio of abnormal to normal goblet cells in WT, *Nod2*$^{-/-}$, *Nod2*$^{-/-}$ Jax, and *Nod2*$^{-/-}$ Jax gavaged with *P vulgatus* mice housed under conventional SPF conditions. (*D*) Quantification of the percentage of CD8+ IELs expressing IFNγ in WT, *Nod2*$^{-/-}$, *Nod2*$^{-/-}$ Jax, and *Nod2*$^{-/-}$ Jax gavaged with *P vulgatus* mice. (*E*) CFUs of *P vulgatus* per mg of stool collected over time in stool of *Nod2*$^{-/-}$ and *Nod2*$^{-/-}$ Jax gavaged with *P vulgatus*. (*E–H*) Quantification of the number of total goblet cells per villus, normal goblet cells per villus, and ratio of abnormal to normal goblet cells in GF *Nod2*$^{-/-}$ mice gavaged with PBS, *P vulgatus,* WT stool and *P vulgatus,* and *Nod2*$^{-/-}$ Jax stool and *P vulgatus*. (*I*) Quantification of the percentage of CD8+ IELs expressing IFNγ in germ-free *Nod2*$^{-/-}$ mice gavaged with PBS, *P vulgatus*, WT stool and *P vulgatus,* and *Nod2*$^{-/-}$ Jax stool and *P vulgatus*. (*J*) CFUs of *P vulgatus* per mg of stool collected over time in stool of GF *Nod2*$^{-/-}$ mice gavaged with *P vulgatus*, WT stool and *P vulgatus,* and *Nod2*$^{-/-}$ Jax stool and *P vulgatus*. (*K*) Quantification of the number of pERK-positive epithelial cells per villus. (*L*) Quantification of the number of normal goblet cells per villus in *Nod2*$^{-/-}$ mice harboring MF (*Nod2*$^{-/-}$ MF) gavaged with PBS and *P vulgatus*. (*M*) Quantification of the percentage of CD8+ IELs expressing IFNγ in *Nod2*$^{-/-}$ MF gavaged with PBS and *P vulgatus*. Representative data from at least 2 independent experiments with n = 3–17 mice/group are shown. At least 25 villi per mouse were quantified for *A–C, F–H,* and *L*. Ordinary 1-way ANOVA with testing for multiple comparisons (Tukey) was performed with *P*-values < .05 shown.

IFN-γ production by CD8+ IELs and goblet cell defects (Figure 6*F–J*). Stool from conventional WT mice resulted in similar abnormalities, indicating that the required microorganisms can also be found in the conventional setting of WT stool (Figure 6*F–J*). Additionally, we found an increase in pERK staining in the small intestinal epithelium of the GF *Nod2*$^{-/-}$ mice reconstituted with stool and *P vulgatus* similar to that of the conventional *Nod2*$^{-/-}$ mice (Figure 6*K*). To further define the requirement of the microbiota, we examined whether intestinal defects can be restored in the

presence of the Oligo-MM12 + FA3 minimal flora, a simplified synthetic microbiota that consists of 15 bacteria species designed to represent dominant phyla in mice.[49,50] GF WT and GF *Nod2*$^{-/-}$ mice that were colonized with Oligo-MM12 +FA3[51] did not display any intestinal abnormalities when gavaged with *P vulgatus* (Figure 6*L* and *M*). Thus, additional members of the microbiota are required for *P vulgatus* mediated defects in *Nod2*$^{-/-}$ mice.

Discussion

Previous studies identified goblet cell defects as a disease feature that distinguishes UC from CD, but these observations focused on colonic goblet cells.[12,13] Our findings link *NOD2* mutations to goblet cell defects in noninflamed ileal tissue that may be a risk factor for disease recurrence and reoperation in patients with CD requiring ileocolic resection. In mouse studies, we show a requirement for complex microbiota in promoting *P vulgatus*-associated effects downstream of signaling through intestinal epithelial MyD88 and TLR4.

Analysis of our cohort revealed that patients harboring *NOD2* risk alleles were diagnosed at a younger age, as others have reported.[18,52–54] Although we did not find a relationship with disease location *per se*, in this small sample size, the trend was in the expected direction. In addition, these patients tended towards having penetrating disease, for which there are conflicting data in the literature.[18] No differences were observed regarding perianal disease, which is in line with prior evidence.[55,56]

Patients with *NOD2* mutations had higher proportions of adverse postoperative disease outcomes. On multivariate analysis, we found a higher risk of subsequent reoperation after initial intestinal resection. This finding echoes data from previous studies, which showed that *NOD2* variants are associated with not only the risk of small bowel resections but also a higher risk of postoperative recurrence of disease after resection, shorter disease-free survival after surgery, higher risk of a second surgery, and shorter interval to next operation.[19,52,57–62] Similarly, a correlation between *NOD2* risk allele carriage and history of intestinal resection was found in the SPARC IBD cohort, providing further validation. Thus, although our study was not powered to dissect contribution of individual alleles as previously reported.[55,63,64] our results are in line with other work showing contribution of *NOD2* risk alleles to disease outcome risks in patients with CD.

P vulgatus and its byproducts are associated with IBD in humans and animal models.[33,34,65–76] However, *P vulgatus* is not always enriched in patient specimens, and there is no consensus on its role in IBD pathogenesis. Although we confirmed the presence of *P vulgatus* in patients with CD who have ileal disease, it was not increased in individuals with *NOD2* risk alleles. Although this may appear contradictory to our findings in mice, there are several limitations that may explain this finding. Our previous work showed that *P vulgatus* abundance is increased in mice in the absence of inflammation, and, in fact, it decreases after the onset of small intestinal inflammation.[33] In the SPARC IBD cohort, the distribution of abundances by phyla suggest similarity to mice after inflammation. Expansion of proteobacteria may contribute to the decreased abundance of other important taxa. In addition, the number of individuals with 2 *NOD2* risk alleles was small, and we were not able to control for small intestinal inflammation status at the time when patients submitted their fecal samples. Thus, some patients may have had small intestinal inflammation and others not, possibly supported by the apparent bimodal distribution of abundance of *P vulgatus* (Figure 2*E*).

Another possibility is that the *P vulgatus* association with *NOD2* is not exclusive. In this context, it is notable that *P vulgatus* required the presence of additional commensal bacteria to exert adverse effects in the *Nod2* knockout mouse model. Certainly, cooperation between species has previously been shown to exert consequences.[77] If multiple species are required, then the presence or absence of one species such as *P vulgatus* may not distinguish patients with IBD from controls in a given study.

Precisely how *P vulgatus* interacts with other commensals to induce TLR-MyD88 signaling, particularly via TLR4, is unknown in our model. *P vulgatus* is one of numerous Gram-negative species. One hypothesis is that cooperation between commensals allows for *P vulgatus* or other Gram-negative species to reach TLRs in the intestinal epithelium. This could occur through degradation of the mucin layer, effectively removing the barrier, or by altering the mucosal microbial niche. Indeed, we previously showed that the mucus-consuming *Akkermansia* is increased in Nod2$^{-/-}$ mice colonized with *P vulgatus* and could contribute to mucus degradation in the setting of *P vulgatus* expansion.[33]

Moreover, TLR-Myd88 signaling has been shown to promote antimicrobial gene expression. In our previous work, we showed that REG3 and other antimicrobial proteins are upregulated in Nod2-deficient mice in the setting of *P vulgatus*-induced dysbiosis.[33] Although REG3 family members are required for barrier protection, we have also previously shown that overproduction can lead to dysbiosis, with reduction of protective species and subsequent propensity towards inflammation.[20] Thus, *P vulgatus* and other commensals signaling through TLR-Myd88 might generate a feedback loop through antimicrobial gene expression that allow other species to expand or to breach the barrier and thereby promote IEL responses.

Our findings shed light on the complex interplay between 2 innate immune molecules important to intestinal homeostasis, NOD2 and TLR4. Previous work suggests dual roles for TLR4 in both protection from infection and maintenance of homeostasis in the gut. NOD2 inhibits TLR4 signaling in the intestinal epithelium in a mouse model of necrotizing enterocolitis.[78] NOD2 and TLR2/4 also have an antagonistic role in hematopoietic lineage cells, and TLR2/4 stimulation in the absence of NOD2 leads to increased Peyer's patch permeability.[45,46,79,80] Our BM chimera experiments indicate that TLR4 in non-hematopoietic cells mediates the pathologic consequences of NOD2 in hematopoietic cells, providing evidence for crosstalk between these 2 innate immune molecules in different cell types. Our data also corroborate the literature that suggests that unmitigated TLR4 signaling in the intestinal epithelium is

dangerous.[81,82] However, the role of TLR4 in intestinal homeostasis is complex, as complete deficiency has been shown to worsen colitis.[37] These observations may not be at odds with each other. TLR4 could protect from small intestinal disease in the presence of specific microbiota communities when NOD2 signaling is deficient. In addition, although we did not address this possibility in our present study, signaling through other TLRs may be at play, consistent with partial rescue of TLR2-deficient mice by oral administration of the TLR4 ligand LPS.[83] A role for other innate immune sensors could explain how abundant pERK was found throughout the small intestinal epithelium, whereas *Tlr4* expression remained low in *Nod2*$^{-/-}$ mice.

TLR4 is expressed more highly in the colonic epithelium compared with the small intestinal epithelium, raising the question of how it might induce small intestinal changes. TLR4 in the small intestine may serve as a rheostat to control tolerance to gut microbes, which, with its low expression, could be highly sensitive to changes. For example, if NOD2 signaling is intact, TLR4 signaling in the small intestine remains low and/or deactivated. However, colonic TLR4 signaling may contribute to susceptibility to inflammation in *Nod2*$^{-/-}$ mice colonized with *P vulgatus*, which more densely colonizes the colon. Also, microbes from one region have been shown to affect inflammation in the colon, as in the case with certain oral microbes and colitis.[84]

Finally, NSAID exposure has previously been described to associate more with CD than UC, and patients are advised to avoid NSAIDs where possible to limit risks of inflammation because they cause direct mucosal injury.[85] We previously reported localized attachment of intestinal tissue to other organs in *Nod2*-deficient mice after piroxicam treatment, which, along with histology showing transmural inflammation, may be a sign of penetrating disease.[33] Thus, it would be important to determine in a future study whether *NOD2* patients are at specific risk for NSAID-induced disease flares.

This work provides insights into the interactions between host genetics, microbiota, and intestinal epithelial interactions. Although we show presence of *P vulgatus*, goblet cell defects, and increase in small intestine epithelial pERK staining in patients with *NOD2* risk alleles, we do not directly prove that these mechanisms confer risk of postoperative recurrence. Future clinical studies using a prospective design approach could directly address whether goblet cell abnormalities induced by IFNγ-producing IELs are associated with increased risk of disease recurrence in patients after ileocolic resection.[86–91] Such studies could help inform management of patients in the postoperative period, such as risk-stratifying patients based on *NOD2* or goblet cell status to determine who would most benefit from immediate postoperative prophylaxis.

Methods

Human Subjects

ISMMS cohort. We performed a retrospective case-control study to assess the impact of *NOD2* variations in the clinical course of patients with CD who had undergone analysis for *NOD2* polymorphisms. We included patients carrying any of the 3 major CD-associated *NOD2* risk alleles (G908R.rs2066845, R702W.rs2066844, and X1007fs.rs5743293) and controls carrying no *NOD2* risk alleles. The inclusion criteria were: (1) CD diagnosis according to clinical practice guidelines at the time of genotyping; (2) availability of clinical information in our institution's medical record system at baseline; and (3) availability of follow-up data for at least 3 years after genotyping. Data on age at genotyping, age at diagnosis, sex at birth, race, body mass index, smoking status, family history of IBD, disease duration, Montreal classification, medications, surgical history, and postoperative outcomes was retrospectively collected. This study was approved by the Institutional Review Board at the Icahn School of Medicine at Mount Sinai (Protocol 14-00174).

SPARC IBD cohort. The design and implementation of the SPARC IBD cohort has been previously described.[35,36] Briefly, SPARC IBD is a component of the Crohn's and Colitis Foundation's IBD Plexus data exchange platform, wherein patients with IBD are enrolled from sites throughout the United States. Clinical data is collected from electronic health records and case report forms. Patients provide blood and stool samples at enrollment and at the time of a colonoscopy performed as part of usual care. For this study, we included patients with CD who had ileal involvement and either underwent prior ileal resection or no prior bowel resection before the first collected stool sample. Fecal DNA extraction and metagenomics sequencing for this cohort were previously described.[35] The SPARC IBD study is approved by the Institutional Review Board of the University of Pennsylvania.

Human NOD2 Genotyping

Genomic DNA was prepared from frozen blood samples using Qiagen kit. Single nucleotide polymorphisms (SNPs) for *NOD2 Leu1007fsInsC* (rs2066847, SNP13), *R702W* (rs2066844, SNP8) and *G908R* (rs2066845, SNP12) were determined by Taqman Genotyping Master Mix (Life Technologies) protocol using the following primers and probes: (1) *NOD2* SNP8: TTCCTGGCAGGGCTGTTGTC and AGTGGAAGTGCTTGCGGAGG (primers), FCCTGCTCCGGCGCCAGGC and CCTGCTCTGGCGCCAGGCC (probes); (2) *NOD2*-SNP12: ACTCACTGACACTGTCTGTTGACTCT and AGCCACCTCAAGC TCTGGTG (primers), TTTTCAGATTCTGGGGCAACAGAGTG GGT and TTCAGATTCTGGCGCAACAGAGTGGGT (probes), and (3) *NOD2*-SNP13: GTCCAATAACTGCATCACCTACCTAG and CTTACCAGACTTCCAGGATGGTGT (primers); CCTCCT GCAGGCCCCTTGAAA and CCCTCCTGCAGGCCCTTGAAAT (probes).[92,93]

Mice

For all experiments, age- and sex-matched 6- to 12-week-old mice on the C57BL/6J (B6) background were used. For non- GF mouse experiments, animals were produced in a specific pathogen-free (SPF) facility at the New York University (NYU) Grossman School of Medicine. GF B6

and *Nod2*$^{-/-}$ mice were bred and maintained in flexible-film isolators at the NYU Grossman School of Medicine Gnotobiotics Animal Facility as previously described.[51] *Nod2*$^{-/-}$ mice harboring *P vulgatus* were previously described.[33] Heterozygote breeders were used to generate homozygous knockouts and littermate WT controls for experiments. *Nod2*$^{-/-}$ mice without *P vulgatus*, referred to as *Nod2*$^{-/-}$ Jax mice were obtained from The Jackson Laboratory and bred onsite in a manner similar to *Nod2*$^{-/-}$ mice colonized with *P vulgatus* in a separate room to prevent cross-contamination. *MyD88*$^{-/-}$ and *Tlr4*$^{-/-}$ B6 mice were purchased from The Jackson Laboratory and crossed to *Nod2*$^{-/-}$ mice to generate double mutants. Villin-cre mice were previously described.[94] *Nod2*$^{-/-}$*MyD88*$^{fl/fl}$*;Villin-cre* (*Nod2*$^{-/-}$*MyD88*$^{\Delta IEC}$) mice and *Nod2*$^{-/-}$*MyD88*$^{fl/fl}$ littermate controls generated by crossing Cre-positive and Cre-negative mice. *Nod2*$^{-/-}$ mice and *Tlr4*$^{-/-}$ mice were crossed to generate double mutant mice.

Gnotobiotic mice colonized with the Oligo-MM12 + FA3 synthetic microbiota were generated as previously described.[49,51] Briefly, the following bacteria were cultured and gavaged into GF mice with stable colonization over several generations.[51] *Akkermansia muciniphila* YL44 was a gift from Dr K. McCoy (University of Calgary), and it was grown in 0.1% mucin (Sigma-Aldrich), anaerobic, 37 °C. *Bacteroides caecimuris* I48 was from DSMZ and it was grown in brain heart infusion (BHI) (Anaerobe Systems), anaerobic, 37 °C. *Muribaculum intestinale* YL27 (DSMZ) was grown in chopped meat media (Anaerobe Systems), anaerobic, 37 °C. *Turicimonas muris* was a gift from Dr K. McCoy, and it was grown in BHI, anaerobic, 37 °C. Escherichia coli Mt1B1 (DSMZ) was grown in LB (Sigma-Aldrich), aerobic, 37 °C. *Bifidobacterium longum* subsp. animalis YL2 (DSMZ) was grown in BHI, anaerobic, 37 °C. *Staphylococcus xylosus* 33ERD13C (DSMZ) was grown in tryptic soy broth (TSB)-yeast (Sigma Aldrich), aerobic, 37 °C. *Streptococcus danieliae* ERD01G (DSMZ) was grown in TSB-yeast, microaerophilic, 37 °C. *Enterococcus faecalis* KB1 (DMSZ) was grown in TSB-yeast, aerobic, 30 °C. *Acutalibacter muris* KB18 (DSMZ) was grown in BHI, anaerobic, 37 °C. *Clostridium clostridioforme* YL32 (DSMZ) was grown in peptone yeast extract glucose (PYG) (Anaerobe Systems), anaerobic, 37 °C. *Flavinofractor plautii* YL31 (DSMZ) was grown in PYG, anaerobic, 37 °C. *Blautia coccoides* YL58 (DSMZ) was grown in chopped meat media, anaerobic, 37 °C. *Lactobacillus reuteri* I49 (DMSZ) was grown in de Man-Rogosa-Sharpe agar (MRS), microaerophilic, 37 °C. Clostridium innocuum I46 (DSMZ) was grown in chopped meat media or PYG, anaerobic, 37 °C.

All animal studies were approved by the Institutional Animal Care and Use Committee of the NYU Grossman School of Medicine.

Bone Marrow Chimeras

BM chimeras were generated by lethally irradiating 8-week-old female recipient mice (1100 CGy in 2 divided doses) followed by intravenous injection of 5 × 10^6 T-cell-depleted BM cells from donor female mice.[34,48,94]

Phocaeicola vulgatus *Culture, Gavage, and Quantification*

For inoculation into mice, as previously described, *P vulgatus* was streaked from a frozen stock onto selective Bacteroides bile esculin (BBE) agar (Anaerobe systems).[33] Single colonies were used to inoculate PYG broth and grown at 37 ℃ for 48 hours in an anaerobic chamber.[33] Mice were gavaged with 1 × 10^8 colony forming units (CFU) bacteria. Fecal *P vulgatus* was quantified by dilution plating on selective BBE agar (BD) in an anaerobic chamber (AS-580, Anaerobe Systems) at 37 ℃. Colonies of a single color and morphology grew from *Nod2*$^{-/-}$ samples within 24 to 36 hours but not WT samples.[1,34]

Fecal Gavage

Fresh fecal pellets were collected from B6, *Nod2*$^{-/-}$, and *Nod2*$^{-/-}$Jax. Fecal suspensions were prepared with sterile phosphate buffered saline (PBS) and passed through 40-μm strainers. Mice were orally gavaged with 150 μL of fresh fecal suspensions.[48]

Intestinal Epithelial Lymphocyte Preparation

Small intestine (Peyer's patches removed) was cut longitudinally and rinsed in Hanks' Balanced Salt Solution (HBSS). The tissue was washed in HBSS containing HEPES, sodium pyruvate, 5 mM ethylenediaminetetraacetic acid (EDTA), and 1 mM dithiothreitol (DTT) for 15 min to obtain the IEL fraction. The intestines were further washed in HBSS containing HEPES, sodium pyruvate, and EDTA and digested for 20 minutes using Collagenase VIII (Sigma) to obtain the LP fraction. IEL fractions were filtered and fractionated on a Percoll gradient (40% and 80%). The cells at the interphase of the gradient were collected and washed twice with complete RPMI.

IEL Stim and Flow Cytometry

Lymphocytes were stimulated for 4 hours with a cell stimulation cocktail of phorbol 12-myristate 13-acetate (PMA), ionomycin, brefeldin A, and monensin from eBioscience. Stimulated cells were stained with anti-CD3ε PerCP, anti-TCRβ PE-Cy5 or BV510, anti-CD8α PE-Cy7, anti CD4 APC-Cy7, anti- IFNγ APC, anti-IL17 PE, anti-IFN-ɣ AF 488, anti-IL4 APC, and their respective isotype controls from Biolegend. Fixation and permeabilization buffers from Biolegend were used for intracellular cytokine staining, and a fixable live/dead stain from Biolegend was used to exclude dead cells. Flow cytometric analysis was performed on an LSR II (BD Biosciences) and analyzed using FlowJo (TreeStar).

Piroxicam Mouse Experiments

WT and *Nod2*$^{-/-}$ mice were treated with 60 mg/kg piroxicam and 80 mg/kg piroxicam in powdered mouse chow for 7 days each. Mice were euthanized on day 14, and intestinal sections were obtained for histology as below.

Histology

For all studies, quantification of microscopy data was performed in a blinded fashion. For retrospective histological analysis of ileal tissue from patients with CD with ileal involvement and non-IBD controls who had undergone ileal or ileocecal resections at our center, specimens where pathology showed small intestinal margins negative for inflammation by pathologist's read were included. The formalin-fixed paraffin-embedded (FFPE) tissues were obtained. Tissue specimens were fixed in 10% formalin and embedded in paraffin, and 3-μm sections were used for IHC. Sectioning and PAS-Alcian blue staining were performed by the NYU Histopathology Core. Sections were imaged on Nikon Eclipse Ci microscope and scanned. Goblet cells were quantified by counting the total number of abnormal and normal-appearing cells per villus and graphed as individual values.

For MUC2 and pERK staining, IHC was performed using Ventana Discovery Ultra from Roche. This system allows for automated baking, deparaffinization, and cell conditioning. Single staining was performed using the primary antibody (MUC2 antibody [C3] GTX100664 [1:50], GeneTex, and Phospho-p44/42 MAPK (Erk1/2) (Thr202/Tyr204) (D13.14.4E) XP® Rabbit mAb #4370 [1:2000], Cell Signaling Technology). As secondary antibody, Discovery OMNIMap anti-host-HRP from Roche was used, and the signal was obtained using Discovery ChromoMap DAB RUO from Roche (760-2513) (brown signal). Tissues were counterstained with hematoxylin to visualize the nuclei (blue signal). Whole tissue sections on the slide were converted into high-resolution digital data using a NanoZoomer S210 Digital slide scanner (Hamamatsu).

For mouse experiments, intestinal sections were prepared as previously described and summarized as follows:[33,95,96] Murine small intestinal tissue (2 cm of terminal ileum) was cut open lengthwise, pinned on black wax, and fixed in 10% formalin. Tissues were embedded in 3% low melting point agar (Promega). Formalin fixation and paraffin embedding, sectioning, PAS-Alcian blue, hematoxylin and eosin (H&E), or pERK staining, and microscopy was performed by the NYU Histopathology Core. Sections were imaged on a Nikon Eclipse Ci microscope and scanned. Goblet cells were quantified by counting the total number of abnormal and normal-appearing cells per villus and graphed as individual values.

H&E-stained small-intestinal sections of mice treated with piroxicam were used for histopathologic scoring in a blinded fashion by Y.D., as previously described.[34] Each mouse was given an individual cumulative score based on the following criteria: number of focal ulcers (0 = none; 1 = 1; 2 = 2; etc.), number of abscesses (0 = none; 1 = 1; 2 = 2; etc.), the extent of epithelial hyperplasia (0 = none; 1 = elongated villi and crypts; 2 = severe hyperplasia where the crypt villus axis is 2 times higher than the crypt villus axis in untreated mice), the presence of immune infiltrates (0 = none; 1 = pericryptal infiltrates; 2 = submucosal infiltrates), and villus blunting (0 = none; 1–2 = moderate blunting; 3–4 = severe blunting). The presence of macroscopic abnormalities such intestinal bleeding, and/or intestinal perforation in each mouse was also noted.

Statistical Analysis

Concerning human subjects, the endpoints that were compared among exposed individuals (*NOD2* variant) and controls were the need to start advanced therapy (infliximab, adalimumab, certolizumab, vedolizumab, ustekinumab, rizankizumab [biologics]; filgotinib, upadacitinib [small molecules]) during follow-up and the postoperative outcomes (recurrence, need to start advanced therapy following, reoperation, and IBD-related hospitalization). Postoperative recurrence was defined using endoscopy (Rutgeerts score $\geq$i2 for patients with ileocecal resection) or imaging studies (computed tomography or magnetic resonance showing obvious wall thickening, increased mural or peri-mural signal intensity, mural contrast enhancement or signal intensity, stenosis with pre-stenotic dilatation, fistula, abscess, or conglomerate of bowel loops). Reoperation was defined as need for another resection after the first IBD-related surgery.

Continuous variables, non-normally distributed, were summarized as median and IQR, and the Kruskal-Wallis test was applied. Categorical variables were summarized as percentages, and inferential analysis was performed using the χ^2 test. Then, the OR for achieving the outcomes of interest was computed using univariate and multivariate logistic regression, the latter adjusted for age at diagnosis and disease duration. A *P*-value below .05 was considered significant for all analysis. Data was analyzed using IBM SPSS Statistics, version 29.0.

For microbiome analyses, within-sample similarity was assessed by abundance-adjusted counts per taxa (Shannon diversity). Between-sample similarity was assessed by Bray-Curtis and Jaccard distances, and community-level differences between groups were assessed using the permutational multivariate analysis of variance (ANOVA) test. The abundance of genes and taxa were analyzed at a community level using pairwise distance between samples and visualized with principal coordinates analysis. Linear mixed-effects models were used to detect differences in log2-transformed taxon abundance between sample groups. *P* values from multiple testing procedures were corrected to control for a specified false discovery rate (FDR) with Benjamini-Hochberg method. FDR $<$.1 was considered statistically significant. To assess surgical status as a confounder of the associations between *NOD2* risk allele status and the microbiome composition, we used a mixed effects linear model with *NOD2* risk allele status, surgical status, and microbiome composition to assess change in the beta coefficient for the association of *NOD2* risk allele status with the measure of the microbiome.

For mouse experiments, analysis was performed using GraphPad Prism v.9. An unpaired 2-tailed *t*-test was used to evaluate differences between two groups. An ANOVA with the Holm-Sidak multiple comparisons test was used to evaluate experiments involving multiple groups. For experiments requiring nonparametric analyses, the Wilcoxon-

Mann-Whitney test or Kruskal-Wallis with Dunn's multiple comparisons test were applied.

Supplementary Material

Note: To access the supplementary material accompanying this article, visit the full text version at https://doi.org/10.1016/j.jcmgh.2025.101533.

References

1. Ramanan D, Cadwell K. Intrinsic defense mechanisms of the intestinal epithelium. Cell Host Microbe 2016; 19:434–441.
2. Valdes AM, Walter J, Segal E, Spector TD. Role of the gut microbiota in nutrition and health. BMJ 2018;361:k2179.
3. Odenwald MA, Turner JR. The intestinal epithelial barrier: a therapeutic target? Nat Rev Gastroenterol Hepatol 2017;14:9–21.
4. Chang JT. Pathophysiology of inflammatory bowel diseases. N Engl J Med 2020;383:2652–2664.
5. Wong SY, Cadwell K. There was collusion: microbes in inflammatory bowel disease. PLoS Pathog 2018;14: e1007215.
6. Roda G, Chien Ng S, Kotze PG, et al. Crohn's disease. Nat Rev Dis Primers 2020;6:22.
7. Buisine MP, Desreumaux P, Debailleul V, et al. Abnormalities in mucin gene expression in Crohn's disease. Inflamm Bowel Dis 1999;5:24–32.
8. Buisine MP, Desreumaux P, Leteurtre E, et al. Mucin gene expression in intestinal epithelial cells in Crohn's disease. Gut 2001;49:544–551.
9. Bankole E, Read E, Curtis MA, et al. The relationship between mucins and ulcerative colitis: a systematic review. J Clin Med 2021;10:1935.
10. Breugelmans T, Oosterlinck B, Arras W, et al. The role of mucins in gastrointestinal barrier function during health and disease. Lancet Gastroenterol Hepatol 2022; 7:455–471.
11. Breugelmans T, Arras W, Boen L-E, et al. Aberrant mucin expression profiles associate with pediatric inflammatory bowel disease presentation and activity. Inflamm Bowel Dis 2023;29:589–601.
12. Gersemann M, Becker S, Kübler I, et al. Differences in goblet cell differentiation between Crohn's disease and ulcerative colitis. Differentiation 2009;77:84–94.
13. Singh V, Johnson K, Yin J, et al. Chronic inflammation in ulcerative colitis causes long-term changes in goblet cell function. Cell Mol Gastroenterol Hepatol 2022; 13:219–232.
14. Strugala V, Dettmar PW, Pearson JP. Thickness and continuity of the adherent colonic mucus barrier in active and quiescent ulcerative colitis and Crohn's disease. Int J Clin Pract 2008;62:762–769.
15. He S, Lei P, Kang W, et al. Stiffness restricts the stemness of the intestinal stem cells and skews their differentiation toward goblet cells. Gastroenterology 2023; 164:1137–1151.e15.
16. Cleynen I, Boucher G, Jostins L, et al. Inherited determinants of Crohn's disease and ulcerative colitis phenotypes: a genetic association study. Lancet 2016; 387:156–167.
17. Jostins L, Ripke S, Weersma RK, et al. The International IBD Genetics Consortium (IIBDGC). Host–microbe interactions have shaped the genetic architecture of inflammatory bowel disease. Nature 2012;491:119–124.
18. Kayali S, Fantasia S, Gaiani F, et al. NOD2 and Crohn's disease clinical practice: from epidemiology to diagnosis and therapy, rewired. Inflamm Bowel Dis 2025; 31:552–562.
19. Dang JT, Dang TT, Wine E, et al. The genetics of postoperative recurrence in Crohn disease: a systematic review, meta-analysis, and framework for future work. Crohns Colitis 360 2021;3:otaa094.
20. Jang KK, Heaney T, London M, et al. Antimicrobial overproduction sustains intestinal inflammation by inhibiting Enterococcus colonization. Cell Host Microbe 2023;31:1450–1468.e8.
21. Billmann-Born S, Till A, Arlt A, et al. Genome-wide expression profiling identifies an impairment of negative feedback signals in the Crohn's disease-associated nod2 variant L1007fsinsC. J Immunol 2011; 186:4027–4038.
22. Chamaillard M, Philpott D, Girardin SE, et al. Gene-environment interaction modulated by allelic heterogeneity in inflammatory diseases. Proc Natl Acad Sci U S A 2003;100:3455–3460.
23. Cooney R, Baker J, Brain O, et al. NOD2 stimulation induces autophagy in dendritic cells influencing bacterial handling and antigen presentation. Nat Med 2010; 16:90–97.
24. Kim Y-G, Park J-H, Shaw MH, et al. The cytosolic sensors Nod1 and Nod2 are critical for bacterial recognition and host defense after exposure to toll-like receptor ligands. Immunity 2008;28:246–257.
25. Netea MG, Ferwerda G, De Jong DJ, et al. The frameshift mutation in Nod2 results in unresponsiveness not only to Nod2- but also Nod1-activating peptidoglycan agonists. J Biol Chem 2005;280:35859–35867.
26. Travassos LH, Carneiro LAM, Ramjeet M, et al. Nod1 and Nod2 direct autophagy by recruiting ATG16L1 to the plasma membrane at the site of bacterial entry. Nat Immunol 2010;11:55–62.
27. Watanabe T, Asano N, Murray PJ, et al. Muramyl dipeptide activation of nucleotide-binding oligomerization domain 2 protects mice from experimental colitis. J Clin Invest 2008;118:545–559.
28. Al Nabhani Z, Dietrich G, Hugot JP, Barreau F. Nod2: the intestinal gate keeper. PLoS Pathog 2017;13: e1006177.
29. Nayar S, Morrison JK, Giri M, et al. A myeloid-stromal niche and gp130 rescue in NOD2-driven Crohn's disease. Nature 2021;593:275–281.
30. Al Nabhani Z, Lepage P, Mauny P, et al. Nod2 deficiency leads to a specific and transmissible mucosa-associated microbial dysbiosis which is independent of the mucosal barrier defect. J Crohns Colitis 2016; 10:1428–1436.
31. Frank DN, Robertson CE, Hamm CM, et al. Disease phenotype and genotype are associated with shifts in

intestinal-associated microbiota in inflammatory bowel diseases. Inflamm Bowel Dis 2011;17:179–184.
32. Rehman A, Sina C, Gavrilova O, et al. Nod2 is essential for temporal development of intestinal microbial communities. Gut 2011;60:1354–1362.
33. Ramanan D, Tang MS, Bowcutt R, et al. Bacterial sensor Nod2 prevents inflammation of the small intestine by restricting the expansion of the commensal Bacteroides vulgatus. Immunity 2014;41:311–324.
34. Ramanan D, Bowcutt R, Lee SC, et al. Helminth infection promotes colonization resistance via type 2 immunity. Science 2016;352:608–612.
35. Lewis JD, Daniel SG, Li H, et al. Surgery for Crohn's disease is associated with a dysbiotic microbiome and metabolome: results from two prospective cohorts. Cell Mol Gastroenterol Hepatol 2024;18:101357.
36. Raffals LE, Saha S, Bewtra M, et al. The development and initial findings of a Study of a Prospective Adult Research Cohort with Inflammatory Bowel Disease (SPARC IBD). Inflamm Bowel Dis 2022;28:192–199.
37. Rakoff-Nahoum S, Paglino J, Eslami-Varzaneh F, et al. Recognition of commensal microflora by toll-like receptors is required for intestinal homeostasis. Cell 2004; 118:229–241.
38. Zhang Y, Jiang J, Ji S, et al. The regulatory effect of ERK1/2 signal pathway on production of TNFalpha induced by LPS in mice Kupffer cells. Chin J Traumatol 2001;4:139–142.
39. An H, Yu Y, Zhang M, et al. Involvement of ERK, p38 and NF-kappaB signal transduction in regulation of TLR2, TLR4 and TLR9 gene expression induced by lipopolysaccharide in mouse dendritic cells. Immunology 2002; 106:38–45.
40. Lee SH, Hu L-L, Gonzalez-Navajas J, et al. ERK activation drives intestinal tumorigenesis in Apcmin/+ mice. Nat Med 2010;16:665–670.
41. Frantz AL, Rogier EW, Weber CR, et al. Targeted deletion of MyD88 in intestinal epithelial cells results in compromised antibacterial immunity associated with downregulation of polymeric immunoglobulin receptor, mucin-2, and antibacterial peptides. Mucosal Immunol 2012; 5:501–512.
42. Raetz M, Hwang SH, Wilhelm CL, et al. Parasite-induced TH1 cells and intestinal dysbiosis cooperate in IFN-γ-dependent elimination of Paneth cells. Nat Immunol 2013;14:136–142.
43. Vaishnava S, Yamamoto M, Severson KM, et al. The antibacterial lectin RegIIIgamma promotes the spatial segregation of microbiota and host in the intestine. Science 2011;334:255–258.
44. Watanabe T, Kitani A, Murray PJ, Strober W. NOD2 is a negative regulator of Toll-like receptor 2–mediated T helper type 1 responses. Nat Immunol 2004;5:800–808.
45. Hedl M, Li J, Cho JH, Abraham C. Chronic stimulation of Nod2 mediates tolerance to bacterial products. Proc Natl Acad Sci U S A 2007;104:19440–19445.
46. Kullberg BJ, Ferwerda G, de Jong DJ, et al. Crohn's disease patients homozygous for the 3020insC NOD2 mutation have a defective NOD2/TLR4 cross-tolerance to intestinal stimuli. Immunology 2008;123:600–605.
47. Price AE, Shamardani K, Lugo KA, et al. A map of toll-like receptor expression in the intestinal epithelium reveals distinct spatial, cell type-specific, and temporal patterns. Immunity 2018;49:560–575.e6.
48. Wong SY, Coffre M, Ramanan D, et al. B cell defects observed in Nod2 knockout mice are a consequence of a Dock2 mutation frequently found in inbred strains. J Immunol 2018;201:1442–1451.
49. Brugiroux S, Beutler M, Pfann C, et al. Genome-guided design of a defined mouse microbiota that confers colonization resistance against Salmonella enterica serovar Typhimurium. Nat Microbiol 2016;2:16215.
50. Darnaud M, De Vadder F, Bogeat P, et al. A standardized gnotobiotic mouse model harboring a minimal 15-member mouse gut microbiota recapitulates SOPF/SPF phenotypes. Nat Commu 2021;12:6686.
51. Dallari S, Heaney T, Rosas-Villegas A, et al. Enteric viruses evoke broad host immune responses resembling those elicited by the bacterial microbiome. Cell Host Microbe 2021;29:1014–1029.e8.
52. Kunovsky L, Kala Z, Marek F, et al. The role of the NOD2/CARD15 gene in surgical treatment prediction in patients with Crohn's disease. Int J Colorectal Dis 2019; 34:347–351.
53. Horowitz JE, Warner N, Staples J, et al. Mutation spectrum of NOD2 reveals recessive inheritance as a main driver of early onset Crohn's disease. Sci Rep 2021; 11:5595.
54. Giudici F, Cavalli T, Luceri C, et al. Long-term follow-up, association between CARD15/NOD2 polymorphisms, and clinical disease behavior in Crohn's disease surgical patients. Mediators Inflamm 2021;2021:8854916.
55. Adler J, Rangwalla SC, Dwamena BA, Higgins PD. The prognostic power of the NOD2 genotype for complicated Crohn's disease: a meta-analysis. Am J Gastroenterol 2011;106:699–712.
56. Freire P, Portela F, Donato MM, et al. CARD15 mutations and perianal fistulating Crohn's disease: correlation and predictive value of antibiotic response. Dig Dis Sci 2011; 56:853–859.
57. Alvarez-Lobos M, Arostegui JI, Sans M, et al. Crohn's disease patients carrying Nod2/CARD15 gene variants have an increased and early need for first surgery due to stricturing disease and higher rate of surgical recurrence. Ann Surg 2005;242:693–700.
58. Büning C, Genschel J, Bühner S, et al. Mutations in the NOD2/CARD15 gene in Crohn's disease are associated with ileocecal resection and are a risk factor for reoperation. Aliment Pharmacol Ther 2004;19: 1073–1078.
59. Renda MC, Orlando A, Civitavecchia G, et al. The role of CARD15 mutations and smoking in the course of Crohn's disease in a Mediterranean area. Am J Gastroenterol 2008;103:649–655.
60. Seiderer J, Schnitzler F, Brand S, et al. Homozygosity for the CARD15 frameshift mutation 1007fs is predictive of early onset of Crohn's disease with ileal stenosis, enteroenteral fistulas, and frequent need for surgical intervention with high risk of re-stenosis. Scand J Gastroenterol 2006;41:1421–1432.

61. Seiderer J, Brand S, Herrmann KA, et al. Predictive value of the CARD15 variant 1007fs for the diagnosis of intestinal stenoses and the need for surgery in Crohn's disease in clinical practice: results of a prospective study. Inflamm Bowel Dis 2006;12:1114–1121.
62. Kline BP, Weaver T, Brinton DL Jr, et al. Clinical and genetic factors impact time to surgical recurrence after ileocolectomy for Crohn's disease. Ann Surg 2021; 274:346–351.
63. Jürgens M, Brand S, Laubender RP, et al. The presence of fistulas and NOD2 homozygosity strongly predict intestinal stenosis in Crohn's disease independent of the IL23R genotype. J Gastroenterol 2010;45:721–731.
64. Barreiro M, Núñez C, Domínguez-Muñoz JE, et al. Association of NOD2/CARD15 mutations with previous surgical procedures in Crohn's disease. Rev Esp Enferm Dig 2005;97:547–553.
65. Dicksved J, Halfvarson J, Rosenquist M, et al. Molecular analysis of the gut microbiota of identical twins with Crohn's disease. ISME J 2008;2:716–727.
66. Gonzalez CG, Mills RH, Zhu Q, et al. Location-specific signatures of Crohn's disease at a multi-omics scale. Microbiome 2022;10:133.
67. Haller D, Russo MP, Sartor RB, Jobin C. IKK beta and phosphatidylinositol 3-kinase/Akt participate in non-pathogenic Gram-negative enteric bacteria-induced RelA phosphorylation and NF-kappa B activation in both primary and intestinal epithelial cell lines. J Biol Chem 2002;277:38168–38178.
68. Hoentjen F, Tonkonogy SL, Qian BF, et al. CD4(+) T lymphocytes mediate colitis in HLA-B27 transgenic rats monoassociated with nonpathogenic Bacteroides vulgatus. Inflamm Bowel Dis 2007;13:317–324.
69. Huang YL, Chassard C, Hausmann M, et al. Sialic acid catabolism drives intestinal inflammation and microbial dysbiosis in mice. Nat Commun 2015;6:8141.
70. Kathania M, Tsakem EL, Theiss AL, Venuprasad K. Gut microbiota contributes to spontaneous colitis in E3 ligase itch-deficient mice. J Immunol 2020; 204:2277–2284.
71. Machiels K, Sabino J, Vandermosten L, et al. Specific members of the predominant gut microbiota predict pouchitis following colectomy and IPAA in UC. Gut 2017; 66:79–88.
72. Maldonado-Contreras A, Ferrer L, Cawley C, et al. Dysbiosis in a canine model of human fistulizing Crohn's disease. Gut Microbes 2020;12:1785246.
73. Mills RH, Dulai PS, Vázquez-Baeza Y, et al. Multi-omics analyses of the ulcerative colitis gut microbiome link Bacteroides vulgatus proteases with disease severity. Nat Microbiol 2022;7:262–276.
74. Ó Cuiv P, de Wouters T, Giri R, et al. The gut bacterium and pathobiont Bacteroides vulgatus activates NF-κB in a human gut epithelial cell line in a strain and growth phase dependent manner. Anaerobe 2017;47:209–217.
75. Schirmer M, Franzosa EA, Lloyd-Price J, et al. Dynamics of metatranscription in the inflammatory bowel disease gut microbiome. Nat Microbiol 2018;3:337–346.
76. Weiss GA, Grabinger T, Glaus Garzon J, et al. Intestinal inflammation alters mucosal carbohydrate foraging and monosaccharide incorporation into microbial glycans. Cell Microbiol 2021;23:e13269.
77. Rakoff-Nahoum S, Foster KR, Comstock LE. The evolution of cooperation within the gut microbiota. Nature 2016;533:255, 259.
78. Richardson WM, Sodhi CP, Russo A, et al. Nucleotide-binding oligomerization domain-2 inhibits toll-like receptor-4 signaling in the intestinal epithelium. Gastroenterology 2010;139:904–917, 917.e1–6.
79. Frédérick B, Chrystèle M, Ulrich M, et al. Nod2 regulates the host response towards microflora by modulating T cell function and epithelial permeability in mouse Peyer's patches. Gut 2010;59:207.
80. Amendola A, Butera A, Sanchez M, et al. Nod2 deficiency is associated with an increased mucosal immunoregulatory response to commensal microorganisms. Mucosal Immunol 2014;7:391–404.
81. Dheer R, Santaolalla R, Davies JM, et al. Intestinal epithelial toll-like receptor 4 signaling affects epithelial function and colonic microbiota and promotes a risk for transmissible colitis. Infect Immun 2016; 84:798–810.
82. Cario E, Podolsky Daniel K. Differential alteration in intestinal epithelial cell expression of toll-like receptor 3 (TLR3) and TLR4 in inflammatory bowel disease. Infect Immun 2000;68:7010–7017.
83. Takeuchi O, Hoshino K, Kawai T, et al. Differential roles of TLR2 and TLR4 in recognition of Gram-negative and Gram-positive bacterial cell wall components. Immunity 1999;11:443–451.
84. Read E, Curtis MA, Neves JF. The role of oral bacteria in inflammatory bowel disease. Nat Rev Gastroenterol Hepatol 2021;18:731–742.
85. Long MD, Kappelman MD, Martin CF, et al. Role of nonsteroidal anti-inflammatory drugs in exacerbations of inflammatory bowel disease. J Clin Gastroenterol 2016; 50:152–156.
86. Buisson A, Sokol H, Hammoudi N, et al. Role of adherent and invasive Escherichia coli in Crohn's disease: lessons from the postoperative recurrence model. Gut 2023; 72:39–48.
87. Fumery M, Seksik P, Auzolle C, et al. Postoperative complications after ileocecal resection in Crohn's disease: a prospective study from the REMIND Group. Am J Gastroenterol 2017;112:337–345.
88. Sokol H, Brot L, Stefanescu C, et al, REMIND Study Group Investigators. Prominence of ileal mucosa-associated microbiota to predict postoperative endoscopic recurrence in Crohn's disease. Gut 2020; 69:462–472.
89. Ahmed T, Rieder F, Fiocchi C, Achkar J-P. Pathogenesis of postoperative recurrence in Crohn's disease. Gut 2011;60:553–562.
90. Hammoudi N, Sachar D, D'Haens G, et al. Outcomes and endpoints of postoperative recurrence in Crohn's disease: systematic review and consensus conference. J Crohns Colitis 2024;18:943–957.
91. Battat R, Sandborn WJ. Advances in the comprehensive management of postoperative Crohn's disease. Clin Gastroenterol Hepatol 2022;20:1436–1449.

92. Chen E, Chuang LS, Giri M, et al. Inflamed ulcerative colitis regions associated with MRGPRX2-mediated mast cell degranulation and cell activation modules, defining a new therapeutic target. Gastroenterology 2021;160:1709–1724.
93. Hampe J, Grebe J, Nikolaus S, et al. Association of NOD2 (CARD 15) genotype with clinical course of Crohn's disease: a cohort study. Lancet 2002; 359:1661–1665.
94. Matsuzawa-Ishimoto Y, Shono Y, Gomez LE, et al. Autophagy protein ATG16L1 prevents necroptosis in the intestinal epithelium. J Exp Med 2017;214:3687–3705.
95. Cadwell K, Liu JY, Brown SL, et al. A key role for autophagy and the autophagy gene Atg16l1 in mouse and human intestinal Paneth cells. Nature 2008;456:259–263.
96. Cadwell K, Patel KK, Maloney NS, et al. Virus-plus-susceptibility gene interaction determines Crohn's disease gene Atg16L1 phenotypes in intestine. Cell 2010; 141:1135–1145.

Received July 30, 2024. Accepted May 5, 2025.

Correspondence
Address correspondence to: Serre-Yu Wong, One Gustave L. Levy Place, Box 1069, New York, New York, 10029. e-mail: serre-yu.wong@mountsinai.org.

Acknowledgments
The authors thank the Biorepository and Pathology CoRE at the Icahn School of Medicine at Mount Sinai for their contribution to histology and immunohistochemistry studies. The authors acknowledge the contributions of the SPARC IBD investigators: Richa Shukla, MD (Baylor College of Medicine), Themistocles Dassopoulos, MD (Baylor Scott & White), Josh Korzenik, MD (Brigham & Women's Hospital), Scott Snapper, MD, PhD (Brigham & Women's Hospital), Satya Kudara, MD (Indiana University), Laura Raffals, MD (Mayo Clinic), Manreet Kaur, MD (Mayo Clinic Arizona), Poonam Beniwal-Patel, MD (Medical College of Wisconsin), Ray Cross, MD (Mercy Medical Center), David Hudesman, MD (NYU Langone Medical Center), Mazer Ally, MD (Scripps Healthcare), Gauree Konijeti, MD (Scripps Healthcare), Rebecca Matro, MD (Scripps Healthcare), Kirk Russ, MD (University of Alabama), Kara De Felice, MD (University of Cincinnati), Joel Pekow, MD (University of Chicago), Sushila Dalal, MD (University of Chicago), Sheldon Lidofsky, MD (University Gastroenterology), Lauren George, MD (University of Maryland), Shrinivas Bishu, MD (University of Michigan), Meena Bewtra, MD, MPH, PhD (University of Pennsylvania), James Lewis, MD, MSCE (University of Pennsylvania), Richard Duerr, MD (University of Pittsburgh), Sumona Saha, MD, MS (University of Wisconsin), Freddy Caldera, DO, MS (University of Wisconsin), Elizabeth Scoville, MD, MSCI (Vanderbilt University), Parakkal Deepak, MBBS, MS (Washington University). The authors thank all patients whose data were included in this manuscript, without whom this research would not be possible.

CRediT Authorship Contributions
Serre-Yu Wong, MD, PhD (Conceptualization: Lead; Data curation: Lead; Formal analysis: Equal; Funding acquisition: Equal; Investigation: Lead; Methodology: Lead; Supervision: Equal; Visualization: Lead; Writing – original draft: Lead; Writing – review & editing: Lead)
Maria Manuela Estevinho, MD (Data curation: Equal; Formal analysis: Equal; Investigation: Equal; Methodology: Supporting; Visualization: Equal; Writing – original draft: Supporting; Writing – review & editing: Equal)
Thomas Heaney (Investigation: Equal; Visualization: Supporting; Writing – review & editing: Equal)
Allison A. Marshall (Data curation: Equal; Investigation: Equal; Writing – review & editing: Equal)
Elisabeth Giselbrecht (Data curation: Supporting; Investigation: Equal; Writing – review & editing: Equal)
Scott G. Daniel, PhD (Data curation: Equal; Formal analysis: Equal; Investigation: Equal; Methodology: Equal; Visualization: Equal; Writing – review & editing: Supporting)
Chaoting Zhou (Data curation: Equal; Formal analysis: Equal; Investigation: Equal; Methodology: Equal; Visualization: Equal; Writing – review & editing: Supporting)
Adriana Rosas-Villegas (Investigation: Equal; Visualization: Supporting; Writing – review & editing: Equal)
Kyung Ku Jang (Investigation: Supporting; Writing – review & editing: Equal)
Yi Ding (Data curation: Supporting; Formal analysis: Equal; Investigation: Equal; Writing – review & editing: Equal)
Huaibin Mabel Ko (Investigation: Equal; Writing – review & editing: Equal)
John D. Paulsen (Investigation: Supporting; Writing – review & editing: Equal)
Hairu Yang (Investigation: Supporting; Writing – review & editing: Supporting)
Kyle Bittinger (Methodology: Equal; Supervision: Equal; Writing – review & editing: Supporting)
Judy H. Cho (Methodology: Equal; Resources: Equal; Supervision: Equal; Writing – review & editing: Equal)
James D. Lewis (Methodology: Equal; Resources: Equal; Supervision: Equal; Writing – review & editing: Supporting)
Deepshika Ramanan (Conceptualization: Equal; Formal analysis: Equal; Investigation: Equal; Methodology: Equal; Writing – review & editing: Equal)
Ken Cadwell (Conceptualization: Equal; Funding acquisition: Lead; Methodology: Lead; Project administration: Lead; Resources: Lead; Supervision: Lead; Writing – original draft: Equal; Writing – review & editing: Equal)

Conflicts of interest
These authors disclose the following: Serre-Yu Wong reports research contract with Takeda/Trinetx; and advisory board for BMS. Ken Caldwell has consulted for or received honoraria from Puretech Health, Genentech, and Abbvie; and is an inventor on United States patent 10,722,600 and provisional patent 62/935,035 and 63/157,225. The remaining authors disclose no conflicts.

Funding
Serre-Yu Wong has received an American College of Gastroenterology Clinical Research Pilot Award for this work and a Career Development Award from the Crohn's and Colitis Foundation. Ken Caldwell reports National Institutes of Health grant AI130945. James D. Lewis reports support from the Biomedical Data Science Core of the Center for Molecular Studies in Digestive and Liver Diseases (P30DK050306) and the Penn-CHOP Microbiome Center.

Data Availability
The datasets generated during and/or analyzed during the current study are available from the corresponding author on reasonable request.